Vibration Analysis of Tension Stiffened Structures

An internship report submitted

in partial fulfillment for the award of the degree of

Bachelor of Technology

in

Aerospace Engineering

by

Aditya Kumar Shahi (SC21B005)

Department of Aerospace Engineering

Indian Institute of Space Science and Technology

Thiruvananthapuram, India

July 2024

Certificate

This is to certify that the internship report titled ***Vibration Analysis of Tension Stiffened Structures*** submitted by **Aditya Kumar Shahi (SC21B005)**, to the Indian Institute of Space Science and Technology, Thiruvananthapuram, in partial fulfillment for the award of the degree of **Bachelor of Technology** in **Aerospace Engineering** is a bona fide record of the original work carried out by him under my supervision. The contents of this internship report, in full or in parts, have not been submitted to any other Institute or University for the award of any degree or diploma.

Mr Shanbhag Sushanth Suresh
Scientist/ Engineer SC, CVAD/SDEG/STR, VSSC

Dr. Anup S, Ph.D
Professor, Department of Aerospace Engineering, IIST

Place: Thiruvananthapuram
Date: 26/07/2024

भारत सरकार
अन्तरिक्ष विभाग
विक्रम साराभाई अन्तरिक्ष केन्द्र
तिरुवनन्तपुरम - 695 022, भारत
दूरभाष : 0471 - 2562444 / 2562555
फैक्स : 0471 - 2705345

Government of India
Department of Space
Vikram Sarabhai Space Centre
Thiruvananthapuram - 695 022, India
Telephone : 0471-2562444 / 2562555
Fax : 0471-2705345

CERTIFICATE

This is to certify that the internship report entitled "Vibration Analysis of Tension Stiffened Structures" submitted by **Aditya Kumar Shahi (SC21B005)** studying at Indian Institute of Space Science and Technology, Thiruvananthapuram, towards the partial fulfilment of the requirements for the award of the degree of Bachelor of Technology in Aerospace Engineering is a bonafide record of the internship work carried out by him under my supervision at the Composites and Viscoelastic Analysis Division (CVAD) at Vikram Sarabhai Space Centre (VSSC), ISRO, Trivandrum during the period for June 2024 to August 2024. The contents of this report have not been submitted elsewhere for the award of any degree or diploma.

Shanbhag Sushanth Suresh
Scientist / Engineer SC
Composite Structures Section (CSS)
Composites and Viscoelastic Analysis Division (CVAD)
Structural Design and Engineering Group (SDEG)
Structural Engineering Entity (STR), VSSC, ISRO

Date: 19/08/2024

Place:Office Seal

Declaration

I declare that this internship report titled ***Vibration Analysis of Tension Stiffened Structures*** submitted in partial fulfillment for the award of the degree of **Bachelor of Technology** in **Aerospace Engineering** is a record of the original work carried out by me under the supervision of **Mr. Shanbhag Sushanth Suresh**, and has not formed the basis for the award of any degree, diploma, associateship, fellowship, or other titles in this or any other Institution or University of higher learning. In keeping with the ethical practice in reporting scientific information, due acknowledgments have been made wherever the findings of others have been cited.

Place: Thiruvananthapuram

Date: 26/07/2024

Aditya Kumar Shahi (SC21B005)

Acknowledgements

I would like to express my heartfelt gratitude to my guide,**Mr. Shanbhag Sushanth Suresh** Scientist/Engineer SC, CVAD/SDEG/STR at VSSC, for his invaluable guidance and support throughout this internship. His profound knowledge and expertise in the field of vibrations and structural dynamics provided me with the necessary insights to tackle complex problems and achieve my research objectives. His constant encouragement and constructive feedback were instrumental in enhancing the quality of my work.

I am equally grateful to my internal guide, **Dr. Anup S**, Professor of the Aerospace Engineering Department, Indian Institute of Space Science and Technology, Thiruvananthapuram. His academic mentorship and continuous support were vital in shaping the direction of my research. Dr. Anup's deep understanding of aerospace engineering principles and his commitment to academic excellence inspired me to push the boundaries of my knowledge and skills.

I would also like to extend my appreciation to the faculty and staff of the Aerospace Engineering Department at IIST for providing an enriching academic environment and the necessary resources for my research.

Thank you all for your guidance, support, and motivation, which have been pivotal in the successful completion of this internship.

Aditya Kumar Shahi (SC21B005)

Abstract

I conducted a thorough investigation of membrane vibrations and single degree of freedom (SDOF) vibrations for both linear and nonlinear systems during my internship. The two primary components of my research were the analysis of SDOF systems and membrane vibrations.

SDOF System Analysis : This section begins with a study of linear SDOF systems, where the differential equation was solved for both the damping and non-damping cases where there was no external force. The displacement versus time and phase portrait findings were plotted using MATLAB software. In all situations, shape of phase portraits were also examined. Additionally, amplitude dependence was determined with respect to beginning displacement, initial velocity, and angular velocity.

Stiffness was adjusted in nonlinear SDOF systems to create nonlinearity; for positive displacement, it was always positive, and for negative displacement, it was 0. Equations were solved in MATLAB, and the phase portrait and displacement vs. time results were shown. MATLAB's FFT was utilised to determine the system's inherent frequencies. Both forced and free vibrations were covered in these two examples as well.

Vibrations in Membranes: This section of the study concentrated on the free vibration of circular, elliptical, and rectangular membranes. In MATLAB, analytical and numerical solutions were generated, and the outcomes were contrasted. Additionally, the importance of tension in determining stiffness was covered. Next, nonlinear vibration was also noted, with impact loads being the source of the nonlinearity. Plotting of the analytical results was done in MATLAB using the Von Karman theory, D'Alembert's principle, and the KBM perturbation method.

This internship improved my theoretical knowledge of vibrations and showed me how to use them in real-world situations. The study's findings are beneficial to domains involving tensioned stiffend structures.

Contents

List of Figures

List of Tables

Nomenclature

m : Mass of the object
k : Stiffness constant
c : Damping constant
ω : Natural frequency
A : Amplitude of oscillation
ζ : Damping ratio
ω_d : Damped natural frequency
$w(x, y, t)$: Transverse displacement of a rectangular membrane T_x: tension in x direction and
T_y: tension in y direction
ρ : Mass per unit area of the membrane
$w(r, \theta, t)$: Transverse displacement of a circular membrane
T_r: radial tension
T_θ: circumferential tensions

Chapter 1

1.1 Introduction

Numerous applications in science and engineering depend on the knowledge of vibration. Through performance optimisation, these findings and analysis support engineers in their study of dynamic loads, behaviour prediction of systems under dynamic load, and assurance of safety and dependability. SDOF membranes were the subject of these studies from both a linear and nonlinear perspective.

The foundation for comprehending vibration phenomena is SDOF systems, particularly linear SDOF. We frequently assume small oscillations in this situation, for which linear approximations hold, since we know that the restoring force in linear SDOF systems is precisely proportional to displacement. Responses to these systems can be easily predicted because they have been thoroughly examined and researched. It has been determined how mass, stiffness, and damping properties affect system dynamics. However, in the real world, a system's behaviour is nonlinear, and linear proportionality ceases with displacement. Systems respond differently to dynamic loads and become more complicated and unpredictable.

This work examines the nonlinearity resulting from variations in stiffness. Here, nonlinearity is introduced by setting stiffness to zero for negative displacement and constant for positive displacement. Such phenomenon is seen in tension-stiffening devices, such as parachutes, where there is no restoring force when the force becomes compression. Comprehending the dynamic response of these systems is essential for developing parts that can endure intricate loading scenarios without experiencing catastrophic failure.

The report's other section is devoted to membranes. membrane vibration in both linear and nonlinear situations. Thin, flexible materials called membranes are used in many different engineering applications. It has been researched how the stiffness of a membrane depends on tensions and how it varies from other structural components like beams and shells. Membranes are a common sight in everyday objects like cricket nets, parachutes, and emergency evacuation systems. In the final section of this document, nonlinear membrane vibration is also examined. Analytical formulas for displacement, amplitude, and frequency have been derived along with the cause of non-linearity.

The study of membrane vibrations is particularly essential in real life because of its many applications. This work attempts to close the gap between theoretical models and practical implementations by contributing to the behaviour of membrane under dynamic strain.

Chapter 2

Literature Review

2.1 Literature Survey

I have read a lot about the study of SDOF and membrane vibration in the literature, which has given me a solid foundation for this investigation. These are the few research papers that I have included in my internship's literature review.

1.Added Mass of a Membrane Vibrating at Finite Amplitude

This paper [1] provides information on the phenomenon of additional mass that enters the picture and influences membrane vibration properties at finite amplitudes. The impact of additional mass on the membrane's modes and natural frequency is thoroughly examined in this research. The findings presented in this work are significant in situations when it is not possible to assume that the vibration's amplitude is infinitesimally small.

2. Impact-Induced Non linear Damped Vibration of Fabric Membrane Structure: Theory, Analysis, Experiment and Parametric Study

This study [2] discusses the nonlinear vibration of a membrane. Impact on fabric membrane structures results in a nonlinear effect. Numerous methods, such as the von Karman approach and the KBM perturbation methodology, have been used to solve nonlinear membrane vibrations analytically. The importance of nonlinearities and damping effects in fabric membrane design and analysis is discussed in this work. I did not do a direct comparison; instead, I generated solely analytical results, not numerical ones, and discovered that my results and the paper's results were nearly identical.

3.Solution for Free Vibration Problem of Membrane with Unequal Tension in Two Directions

This study [3] focusses on the free vibration of membranes with fixed edges that have rectangular, circular, and elliptical shapes. Analytical methods were used to produce the results, which were then compared to data from other approaches and the error was calculated. This paper exhibits both constant and unequal tension in both directions. This paper also produced an expression for the mode shape and an expression for the angular frequency. I developed the paper's results analytically and numerically, then I compared them. The foundation for comprehending membrane vibration is provided in this study.

All of these publications aided in my comprehension of SDOF systems and membrane vibration, as well as in helping me achieve the outcomes I needed for my internship. This paper's findings and insights are intended to further investigate the dynamic behaviour of membranes and SDOF systems under diverse circumstances.

Chapter 3

Methodology

The methodology adopted for the project work is as shown in 3.1 :

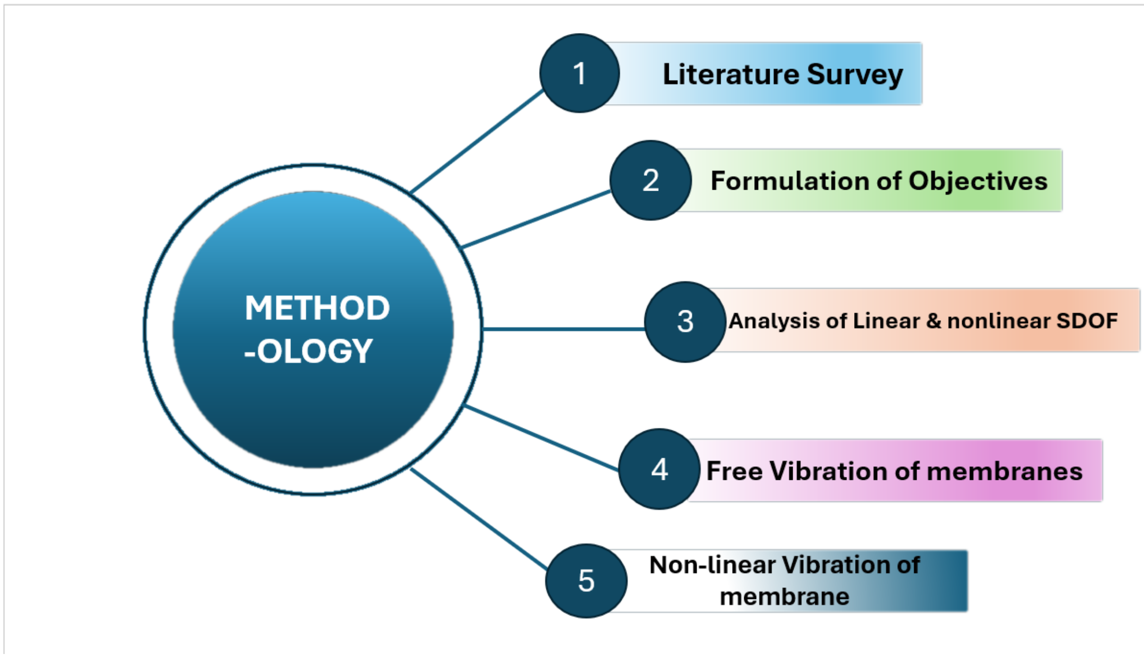

Figure 3.1: Flow Chart of Methodology of the Project

During my internship, I used a methodical approach to investigate and assess membrane free vibrations as well as vibrations with a single degree of freedom (SDOF). This work's technique is divided into 5 steps, which are explained below:

3.1 Review of Literature

During the initial phase, I exclusively concentrated on conducting a literature review. I have out a thorough review of the literature on subjects like membrane vibration. Understanding what was happening theoretically and how to proceed from theoretical to analytical to numerical results required completing this phase. The papers listed below were examined for this internship's work:

- *"Added Mass of a Membrane Vibrating at Finite Amplitude [1]"*: How added mass have impact on vibration in the case of finite amplitudes.
- *"Impact-Induced Nonlinear Damped Vibration of Fabric Membrane Structure: Theory, Analysis, Experiment and Parametric Study [2]"*: This study provided non linear vibration and also provided many analytical method for derivations of non linear vibrations of membrane
- *"Solution for Free Vibration Problem of Membrane with Unequal Tension in Two Directions" by Qian Guo-zhen [3]*: This paper was crucial in understanding about the behaviour of free vibration of membrane in case of unequal tension in both directions.

3.2 Formulation of Objectives

The study objectives for this work were developed using the insights literature survey as a guide. These goals guided my research strategy and helped me achieve my paper's objective.The main goals were as follows:

- Analysing the linear and nonlinear behavior of SDOF systems.
- Analysing the free vibration of membranes with different ahapes.
- Comparison of analytical and numerical results to validate the models.
- Studying the impact of variable tension caused by impact load on membrane vibrations.

3.3 Analysis of Linear & Nonlinear SDOF

A thorough examination of both linear and nonlinear SDOF systems was carried out in the third stage:

- **Linear SDOF**: This section included the analysis of linear SDOF systems with and without damping. The ODE solver in MATLAB was utilised to solve the equations of motion. The behaviour of the system was visualised through the plotting of the phase portrait and displacement versus time graphs. The phase portrait's motivations were likewise explored and supported.

- **Nonlinear SDOF**: This analysis looked at nonlinear SDOF. Variable stiffness, with a positive constant for positive displacement and a zero for negative displacement, was the source of nonlinearity. Two scenarios—forced and free vibration—were discussed. The system grew increasingly sophisticated, therefore the natural frequency of the system was ascertained using FFT. Impact of variables like mass, spring constant, damping constant on natural frequency was also discussed.

3.4 Free Vibration of Membranes

The fourth step examined the free vibration analysis of variously shaped membranes:

- **Rectangular, Circular, and Elliptic Membranes**: Different graphs were plotted for mode shape estimate for each of the three shapes after the equations were solved analytically and numerically using MATLAB. The system's natural frequency was also computed. Though uneven in both directions, the tension does not change. Analytical results were derived using a variety of unique functions, including Mathieu and Bessel functions.

- **Finite Difference approach**: To solve the numerical equations of membrane vibration, I employed the finite difference approach using forward time and central space approximations. This numerical approach was implemented using MATLAB software, which also produced the numerical results for comparison.

3.5 Non linear vibration of membranes

In this section, I examined the study, came to the same analytical conclusions, and visualised the outcomes using Matlab. Owing to time constraints, I was unable to conduct a numerical analysis; nonetheless, I was able to check the analytical results with those presented in the paper, and they were nearly exact.

Through adherence to this methodical approach, I managed to carry out an extensive and comprehensive investigation, making a significant contribution to the domain of vibration analysis.

Chapter 4

Analysis of Linear single degree of freedom

4.1 Linear Single Degree of Freedom System without Damping

A linear single degree of freedom (SDOF) system without damping is a fundamental model used to describe the dynamics of a wide range of mechanical systems.

4.1.1 Governing Equation

For a linear single degree of freedom (SDOF) system without damping, the governing equation is given by: [4]

$$m\ddot{x} + kx = 0 \tag{4.1}$$

where: m is the mass of the system, k is the stiffness of the system, x is the displacement and $\ddot{x}$ is the acceleration.

4.1.2 Solution of the Governing Equation

To solve this differential equation, we assume a solution of the form:

$$x(t) = A\cos(\omega t) + B\sin(\omega t) \tag{4.2}$$

where:

A and B are constants that can be determined by initial conditions and ω is the natural angular frequency of the system. itemize

4.1.3 Formula for Frequency

The natural angular frequency ω is given by:

$$\omega = \sqrt{\frac{k}{m}} \tag{4.3}$$

4.1.4 Initial Conditions

Assume

$x(0) = x_0$ (initial displacement) and $\dot{x}(0) = v_0$ (initial velocity).

Using these initial conditions to find A and B:

$$\begin{aligned}
&\text{At } t = 0: \quad x(0) = A \implies A = x_0 \\
&\text{Taking the derivative of } x(t): \quad \dot{x}(t) = -A\omega \sin(\omega t) + B\omega \cos(\omega t) \\
&\text{At } t = 0: \quad \dot{x}(0) = B\omega \implies B = \frac{v_0}{\omega}
\end{aligned}$$

Thus, the solution is:

$$x(t) = x_0 \cos(\omega t) + \frac{v_0}{\omega} \sin(\omega t) \tag{4.4}$$

4.1.5 Phase Portrait

A phase portrait is a plot of velocity ($\dot{x}$) versus displacement (x).

From the solution:

$$x(t) = x_0 \cos(\omega t) + \frac{v_0}{\omega} \sin(\omega t) \tag{4.5}$$

$$\dot{x}(t) = -x_0\omega \sin(\omega t) + v_0 \cos(\omega t) \tag{4.6}$$

The parametric equations of the phase portrait can be combined into a single equation by eliminating t.

4.1.6 Ellipse Explanation and Proof

To show that the phase portrait is an ellipse:

$$
\begin{aligned}
(x(t))^2 + \left(\frac{\dot{x}(t)}{\omega}\right)^2 &= \left(x_0 \cos(\omega t) + \frac{v_0}{\omega}\sin(\omega t)\right)^2 + \left(\frac{-x_0\omega \sin(\omega t) + v_0 \cos(\omega t)}{\omega}\right)^2 \\
&= x_0^2 \cos^2(\omega t) + 2x_0\frac{v_0}{\omega}\cos(\omega t)\sin(\omega t) + \left(\frac{v_0}{\omega}\right)^2 \sin^2(\omega t) \\
&\quad + x_0^2 \sin^2(\omega t) - 2x_0\frac{v_0}{\omega}\sin(\omega t)\cos(\omega t) + \left(\frac{v_0}{\omega}\right)^2 \cos^2(\omega t) \\
&= x_0^2(\cos^2(\omega t) + \sin^2(\omega t)) + \left(\frac{v_0}{\omega}\right)^2 (\cos^2(\omega t) + \sin^2(\omega t)) \\
&= x_0^2 + \frac{v_0^2}{\omega^2}
\end{aligned}
$$

Therefore, the phase portrait is an ellipse given by

$$
\frac{x^2}{x_0^2} + \frac{\dot{x}^2}{\omega^2 x_0^2} = 1 \tag{4.7}
$$

as shown in the figure 4.2 and figure 4.1 shows variation of displacement versus time in linear SDOF system without damping.

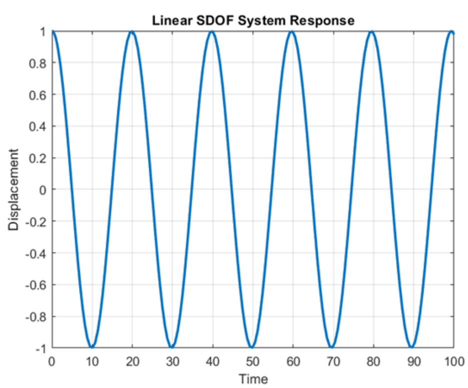

Figure 4.1: Displacement vs time for linear SDOF (without damping)

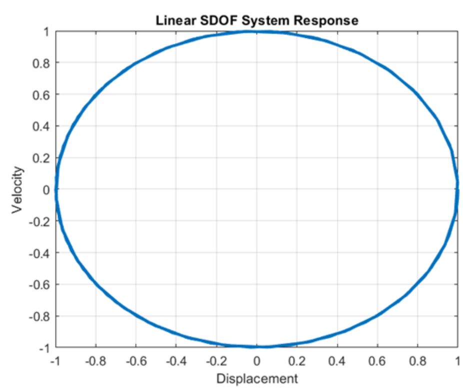

Figure 4.2: Phase portrait for linear SDOF (without damping)

4.1.7 Amplitude of Oscillation

The amplitude of oscillation A is given by the maximum value of $x(t)$. From the solution, the amplitude can be written as:

$$A = \sqrt{x_0^2 + \left(\frac{v_0}{\omega}\right)^2} \tag{4.8}$$

4.1.8 Dependence on Initial Conditions and Angular Frequency

- **Initial displacement** (x_0): As initial displacement increases, amplitude increases.
- **Initial velocity** (v_0): As initial velocity increases, amplitude increases.
- **Angular frequency** (ω): Amplitude of vibration depends on angular frequency in inversely manner. As angular frequency increases, amplitude of the system decreases.

Thus, the amplitude of oscillation is influenced by the initial conditions and the natural frequency of the system.

4.2 Linear Single Degree of Freedom System with Damping

A linear single degree of freedom (SDOF) system with damping introduces the concept of energy dissipation into the dynamics of mechanical systems. In this model, a mass is attached to a spring, and a damping force, often proportional to the velocity of the mass, acts to resist the motion.

4.2.1 Governing Equation

For a linear single degree of freedom (SDOF) system with damping, the governing equation is given by:

$$m\ddot{x} + c\dot{x} + kx = 0 \tag{4.9}$$

where:

m is the mass of the system, c is the damping coefficient, k is the stiffness of the system, x is the displacement, $\dot{x}$ is the velocity and $\ddot{x}$ is the acceleration.

4.2.2 Solution of the Governing Equation

The characteristic equation of the differential equation is:

$$m\lambda^2 + c\lambda + k = 0 \tag{4.10}$$

Solving for λ:

$$\lambda = \frac{-c \pm \sqrt{c^2 - 4mk}}{2m} \tag{4.11}$$

Define the damping ratio ζ and the undamped natural frequency ω_n as:

$$\zeta = \frac{c}{2\sqrt{mk}}, \quad \omega_n = \sqrt{\frac{k}{m}} \tag{4.12}$$

Thus, the characteristic roots can be written as:

$$\lambda_{1,2} = -\zeta\omega_n \pm \omega_n\sqrt{\zeta^2 - 1} \tag{4.13}$$

4.2.3 Damped Frequency

The damped natural frequency ω_d is given by:

$$\omega_d = \omega_n\sqrt{1 - \zeta^2} \tag{4.14}$$

4.2.4 Solutions for Different Damping Cases

- **Underdamped ($\zeta < 1$):** The system oscillates with exponentially decaying amplitude.

$$x(t) = e^{-\zeta\omega_n t}\left(A\cos(\omega_d t) + B\sin(\omega_d t)\right) \tag{4.15}$$

- **Critically damped ($\zeta = 1$):** The system returns to equilibrium without oscillating.

$$x(t) = (A + Bt)e^{-\omega_n t} \tag{4.16}$$

- **Overdamped ($\zeta > 1$):** The system returns to equilibrium without oscillating but more slowly than the critically damped case.

$$x(t) = Ae^{\lambda_1 t} + Be^{\lambda_2 t} \tag{4.17}$$

4.2.5 Initial Conditions

Assume $x(0) = x_0$ (initial displacement) and $\dot{x}(0) = v_0$ (initial velocity).

For the underdamped case ($\zeta < 1$), the constants A and B can be found as follows:
At $t = 0$: $\quad x(0) = x_0 = A$
Taking the derivative of equation 4.15:
$\dot{x}(t) = e^{-\zeta\omega_n t}\left[-\zeta\omega_n(A\cos(\omega_d t) + B\sin(\omega_d t)) + \omega_d(-A\sin(\omega_d t)] + B\cos(\omega_d t))\right.$
At $t = 0$: $\quad \dot{x}(0) = v_0 = -\zeta\omega_n A + \omega_d B \implies B = \frac{v_0+\zeta\omega_n x_0}{\omega_d}$
Thus, the solution for the underdamped case is:

$$x(t) = e^{-\zeta\omega_n t}\left(x_0\cos(\omega_d t) + \frac{v_0 + \zeta\omega_n x_0}{\omega_d}\sin(\omega_d t)\right) \tag{4.18}$$

4.2.6 Phase Portrait

The resulting phase portrait will help us to visualize the behavior of the system and understand the nature of its dynamics.By visualising the phase portrait, we can identify stability, periodicity, and other dynamic properties of the system.

4.2.7 Explanation and Proof of the Spiral Nature

For the underdamped case ($\zeta < 1$), the solution:

$$x(t) = e^{-\zeta\omega_n t}\left(x_0\cos(\omega_d t) + \frac{v_0 + \zeta\omega_n x_0}{\omega_d}\sin(\omega_d t)\right) \tag{4.19}$$

$$\dot{x}(t) = e^{-\zeta\omega_n t}\left[-\zeta\omega_n(x_0\cos(\omega_d t) + \frac{v_0 + \zeta\omega_n x_0}{\omega_d}\sin(\omega_d t)) + \omega_d(-x_0\sin(\omega_d t) + \frac{v_0 + \zeta\omega_n x_0}{\omega_d}\cos(\omega_d t))\right] \tag{4.20}$$

The first term $e^{-\zeta\omega_n t}$ represents an exponentially decaying envelope. Due to this exponential decay term, the amplitude of the system will decrease over time, results in spiral pattern in phase plane as shown in figure 4.4.

4.2.8 Amplitude of Oscillation and Exponential Decay

The amplitude of oscillation at any time t is given by:

$$A(t) = A_0 e^{-\zeta\omega_n t} \tag{4.21}$$

where A_0 is the initial amplitude. The exponential decay is due to the factor $e^{-\zeta\omega_n t}$, which causes the amplitude to decrease over time as shown in figure 4.3.

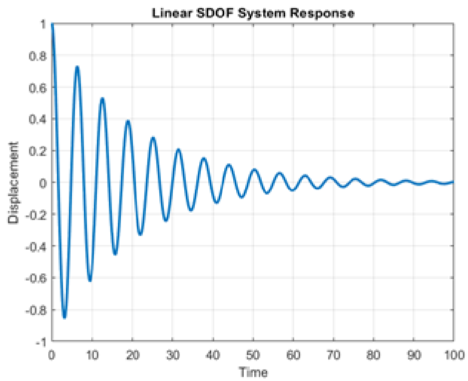

Figure 4.3: Displacement vs time for linear SDOF (with damping)

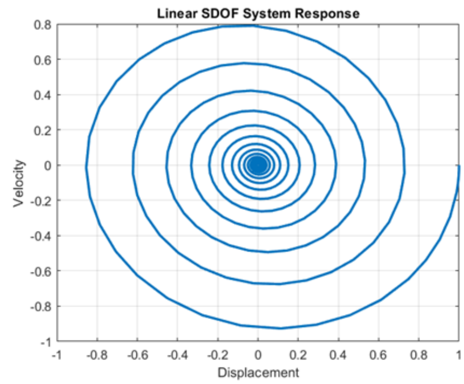

Figure 4.4: Phase Portrait for linear SDOF (with damping)

Chapter 5

Analysis of non linear vibration

Nonlinear SDOF systems are commonly encountered in engineering and physical sciences, where elements may exhibit behavior that deviates from ideal linear assumptions. The book considered for this study is Nonlinear dynamics and Chaos Book by Steven Strogatz. [5]

5.1 Nonlinear Single Degree of Freedom Free Vibration System

5.1.1 Governing Equations

The behavior of the system is defined by two different equations based on the sign of the displacement x. When $x \geq 0$:

$$m\ddot{x} + c\dot{x} + kx = 0 \tag{5.1}$$

When $x < 0$:

$$m\ddot{x} + c\dot{x} = 0 \tag{5.2}$$

for **Positive Displacement ($x \geq 0$):** the material is in tension, and the restoring force kx acts to bring it back to the equilibrium position. **Negative Displacement ($x < 0$):** When the displacement becomes negative, the system exhibit a slack state where there is no restoring force.

5.1.2 Solution for Positive Displacement ($x \geq 0$)

For positive displacement, the system behaves like a typical damped oscillator. The characteristic equation is:

$$m\lambda^2 + c\lambda + k = 0 \tag{5.3}$$

The solutions for λ are:

$$\lambda_{1,2} = \frac{-c \pm \sqrt{c^2 - 4mk}}{2m} \tag{5.4}$$

Define the damping ratio ζ and the undamped natural frequency ω_n as:

$$\zeta = \frac{c}{2\sqrt{mk}}, \quad \omega_n = \sqrt{\frac{k}{m}} \tag{5.5}$$

The damped natural frequency ω_d is:

$$\omega_d = \omega_n \sqrt{1 - \zeta^2} \tag{5.6}$$

The solution for the displacement $x(t)$ is:

$$x(t) = e^{-\zeta \omega_n t} \left(A \cos(\omega_d t) + B \sin(\omega_d t) \right) \tag{5.7}$$

where A and B are constants determined by initial conditions.

5.1.3 Solution for Negative Displacement ($x < 0$)

For negative displacement, the restoring force becomes zero, leaving only the damping force. The equation simplifies to:

$$m\ddot{x} + c\dot{x} = 0 \tag{5.8}$$

Rewriting this equation:

$$\ddot{x} = -\frac{c}{m}\dot{x} \tag{5.9}$$

This is a first-order linear differential equation in $\dot{x}$. Solving it, we get:

$$\dot{x}(t) = \dot{x}_0 e^{-\frac{c}{m}t} \tag{5.10}$$

Integrating once more to find $x(t)$:

$$x(t) = x_0 + \frac{m}{c}\dot{x}_0 \left(1 - e^{-\frac{c}{m}t}\right) \tag{5.11}$$

5.1.4 Behavior Analysis

For **Positive Displacement** ($x \geq 0$)

The system exhibits damped oscillatory behavior. The amplitude of oscillation decreases exponentially over time due to the damping term $e^{-\zeta\omega_n t}$.

For **Negative Displacement** ($x < 0$)

When displacement is negative, there is no restoring force, only damping. As a result, the velocity decays exponentially:

$$\dot{x}(t) = \dot{x}_0 e^{-\frac{c}{m}t} \tag{5.12}$$

The displacement approaches a constant value as time increases:

$$x(t) = x_0 + \frac{m}{c}\dot{x}_0 \left(1 - e^{-\frac{c}{m}t}\right) \tag{5.13}$$

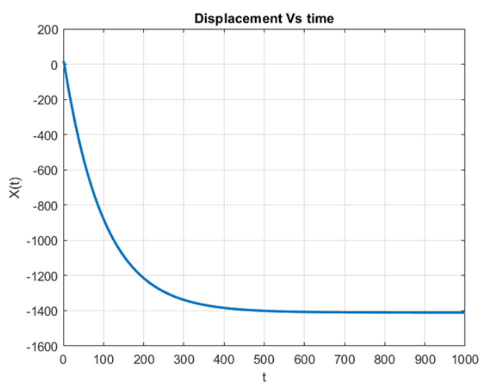

(a) Displacement vs. Time Plot Illustrating Exponential Decay of Oscillation

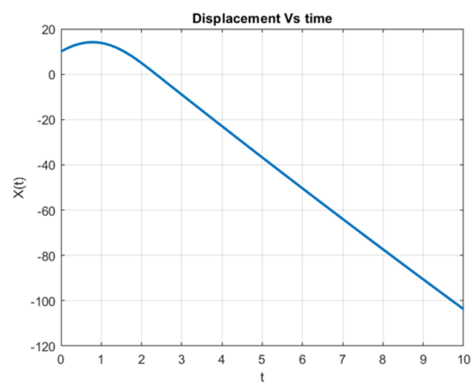

(b) Initial Peak for Positive Displacement (x > 0)

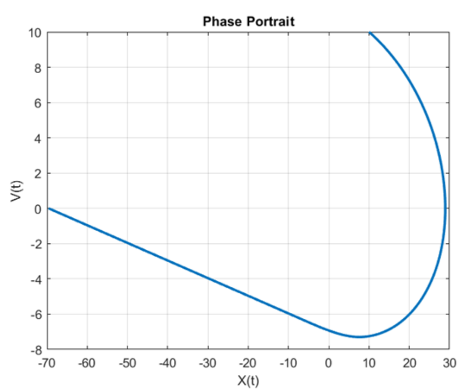

(c) Phase Portrait of non linear free SDOF system

5.1.5 Phase Portrait

For this nonlinear system, the phase portrait will show a spiraling trajectory for positive displacement, because of damped oscillations. For negative displacement, the trajectory will decay exponentially towards the origin, due to absence of restoring force as shown in figure 5.1c.

5.1.6 Oscillatory behaviour of system

The reason of initial peak is, the system is about to oscillate about its equilibrium position because, at first, when the displacement is positive, it behaves like a damped harmonic oscillator, where both restoring and damping forces are present. However, as soon as the displacement becomes negative, the restoring forces disappear and there is only damping force left in the system, which results in non-oscillatory or exponential decay, as shown in the figure 5.1a and 5.1b.

5.2 Nonlinear Single Degree of Freedom Vibration with External Force

5.2.1 Governing Equations

The behavior of the system is defined by two different equations based on the sign of the displacement x.

When $x \geq 0$:

$$m\ddot{x} + c\dot{x} + kx = \sqrt{t} + 100\cos(\sqrt{k/m}t) \tag{5.14}$$

When $x < 0$:

$$m\ddot{x} + c\dot{x} = \sqrt{t} + 100\cos(\sqrt{k/m}t) \tag{5.15}$$

5.2.2 Solution of governing equation

Due to the complexity of the external force, an analytical solution may not be possible, so numerical method have been employed in MATLAB to solve these equations to understand the dynamics of the system.

This equation can be solved using numerical methods to handle the complexity of the external force. 5.2 and 5.3 are only for graphical demonstration how complex a system can be in presence of external force.

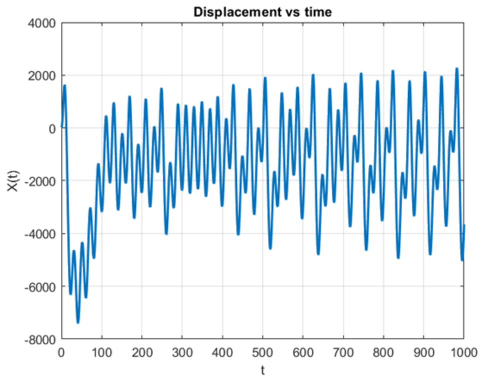

Figure 5.2: Displacement vs time

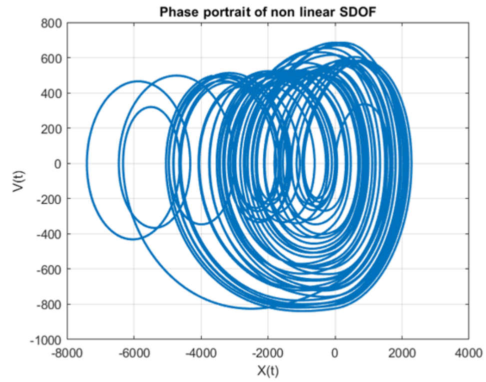

Figure 5.3: Phase Portrait

5.2.3 Fast Fourier Transform (FFT)

To find the natural frequency of the system for such complex system, Fast Fourier Transform (FFT) was performed in MATLAB. The amplitude vs frequency plot was analyzed, and the frequency at which there was a peak in the plot was considered as the natural frequency. This FFT shows excitation of higher harmonics in SDOF systems.

Table 5.1: Natural Frequencies for Different Values of Mass (m) Across Harmonics

Mass (m)	Harmonic 1 (Hz)	Harmonic 2 (Hz)	Harmonic 3 (Hz)
1	158	317	477
5	35	70	105
10	25	50	75

Table 5.2: Natural Frequencies for Different Values of Damping Constant (c) Across Harmonics

Damping Constant (c)	Harmonic 1 (Hz)	Harmonic 2 (Hz)	Harmonic 3 (Hz)
1	50	100	150
0.1	50	100	150
10	50	100	150

5.2.4 Analysis of Frequency Dependence on System Parameters

To determine the dependence of frequency on different system parameters such as stiffness (k), damping (c), mass (m), and initial conditions, I varied one parameter at a time while

Table 5.3: Natural Frequencies for Different Values of Spring Constant (k) Across Harmonics

Spring Constant (k)	Harmonic 1 (Hz)	Harmonic 2 (Hz)	Harmonic 3 (Hz)
1	50	100	150
5	112	224	336
10	158	316	476

keeping the others constant. The results are as follows:

- **Mass (m):** As the mass increases, the natural frequency of the system decreases.
- **Stiffness (k):** As the stiffness increases, the natural frequency of the system increases.
- **Damping (c):** The damping coefficient does not directly affect the natural frequency. However, when include into the external force term, following effects are observed:
  - If c is in the numerator and multiplied with k, the natural frequency increases as c increases.
  - If c is in the denominator, the opposite effect is observed.

Dependence of frequency on various parameters are shown in table 5.1, 5.2 and 5.3.

5.2.5 Plots and Observations

Plots of the phase portrait, displacement vs. time, and amplitude vs. frequency were generated for different cases to observe the system's behavior under various conditions:

5.2.5.1 Varying mass

Given the system parameters:

$$c = 1; x_0 \quad = 10; v_0 = -10; k \quad = \begin{cases} 1 & \text{for } x \geq 0; \\ 0 & \text{for } x < 0; \end{cases}$$

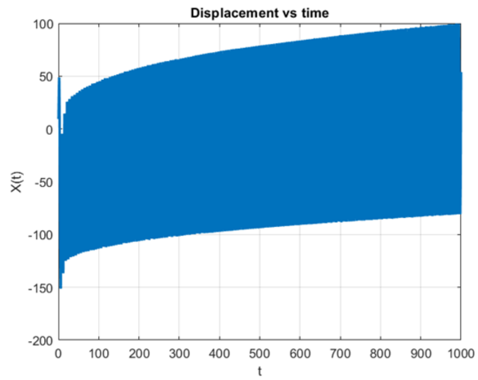

Figure 5.4: Plot of Displacement vs. Time for a Mass of 1 kg

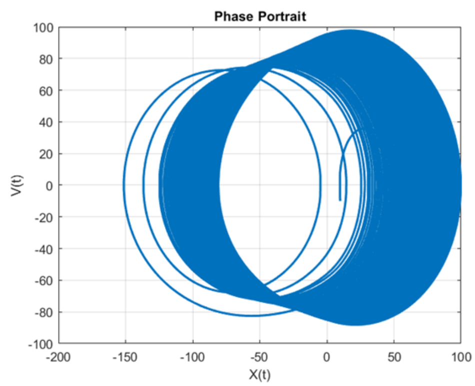

Figure 5.5: Plot of Phase Portrait for a Mass of 1 kg

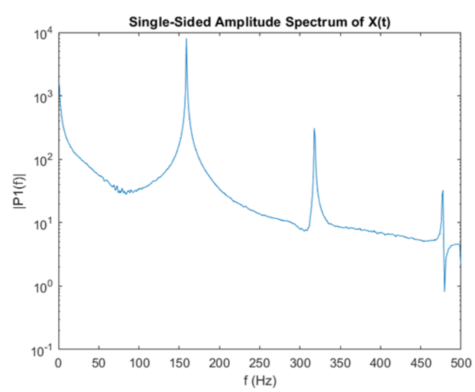

Figure 5.6: Plot of Amplitude vs. Frequency for a Mass of 1 kg

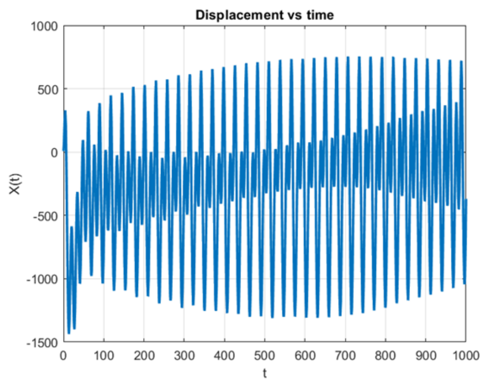

Figure 5.7: Plot of Displacement vs. Time for a Mass of 5 kg

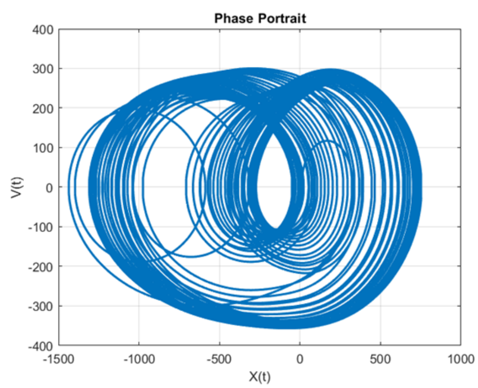

Figure 5.8: Plot of Phase Portrait for a Mass of 5 kg

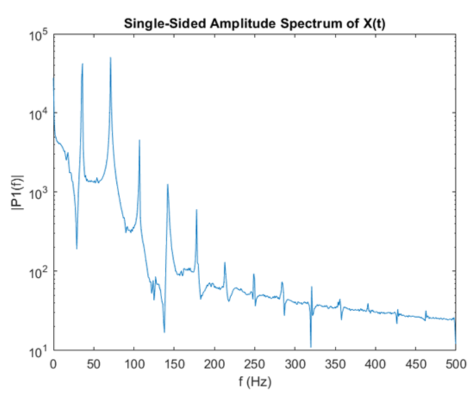

Figure 5.9: Plot of Amplitude vs. Frequency for a Mass of 5 kg

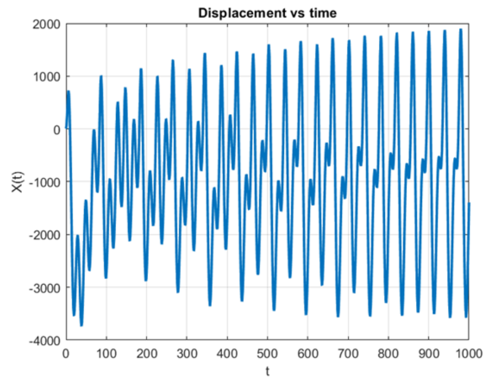

Figure 5.10: Plot of Displacement vs. Time for a Mass of 10 kg

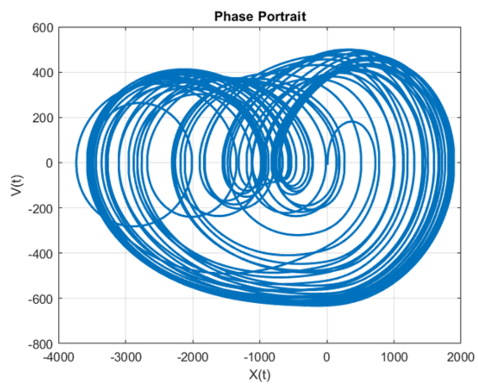

Figure 5.11: Plot of Phase Portrait for a Mass of 10 kg

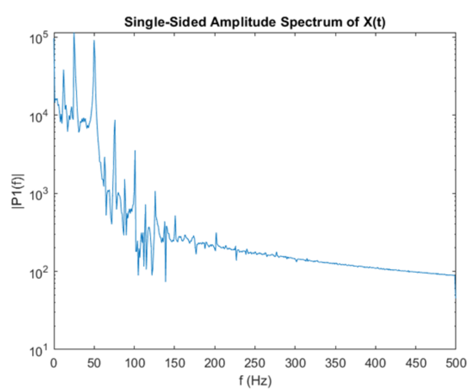

Figure 5.12: Plot of Amplitude vs. Frequency for a Mass of 10 kg

5.2.5.2 Varying Damping constant

Given the system parameters:

$$m = 10; x_0 = 10; v_0 = -10; k = \begin{cases} 1 & \text{for } x \geq 0; \\ 0 & \text{for } x < 0; \end{cases}$$

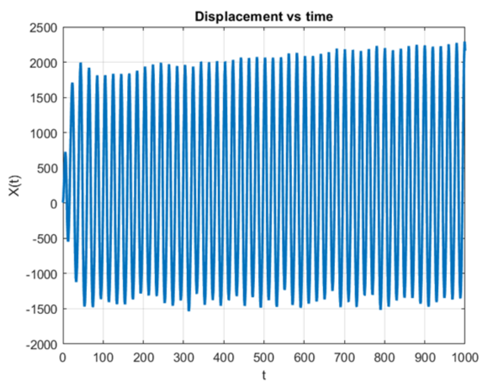

(a) Plot of Displacement vs. Time for c=1

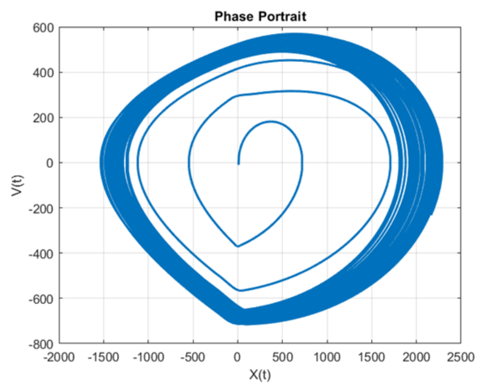

(b) Plot of Phase Portrait for c=1

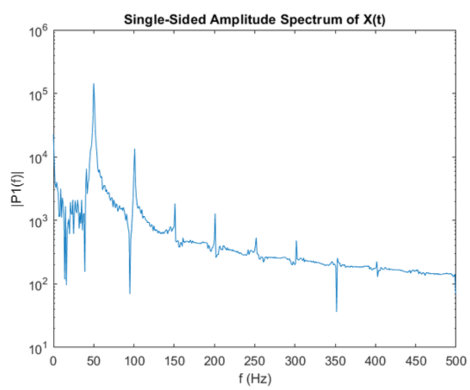

(c) Plot of Amplitude vs. Frequency for c=1

Figure 5.13: Analysis of System Dynamics: Displacement vs. Time, Amplitude vs. Frequency, and Phase Portrait for c=1

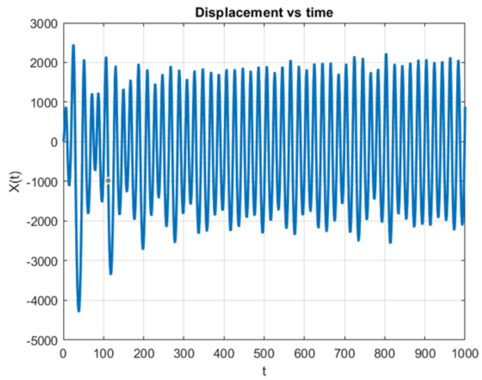

(a) Plot of Displacement vs. Time for c=0.1

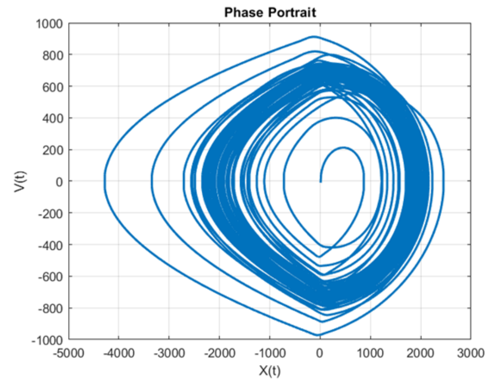

(b) Plot of Phase Portrait c=0.1

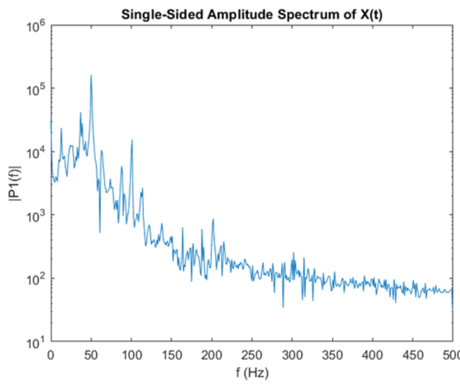

(c) Plot of Amplitude vs. Frequency for c=0.1

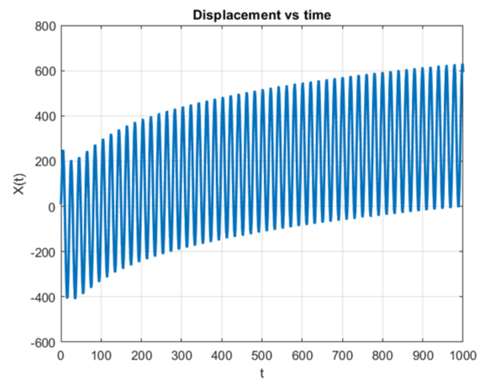

(d) Plot of Displacement vs. Time for c=10

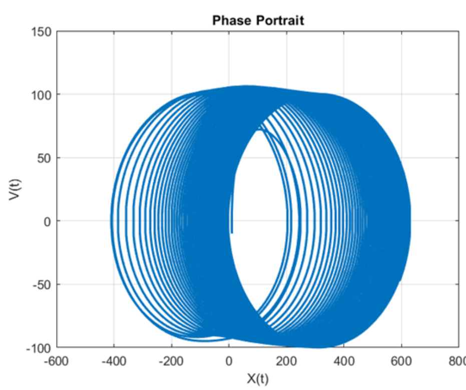

(e) Plot of Phase Portrait for c=10

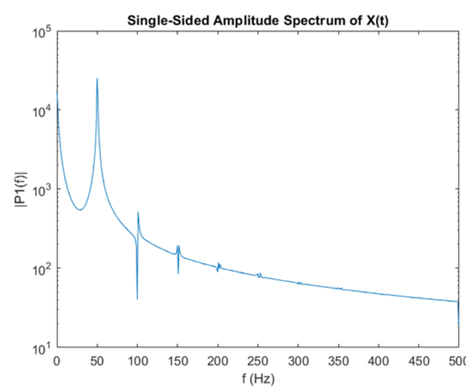

(f) Plot of Amplitude vs. Frequency for c=10

Figure 5.14: Analysis of System Dynamics for c=0.1 and c=10

5.2.5.3 Varying Spring constant

Given the system parameters:

$$m = 10; x_0 \quad = 10; v_0 = -10; c \quad = 1;$$

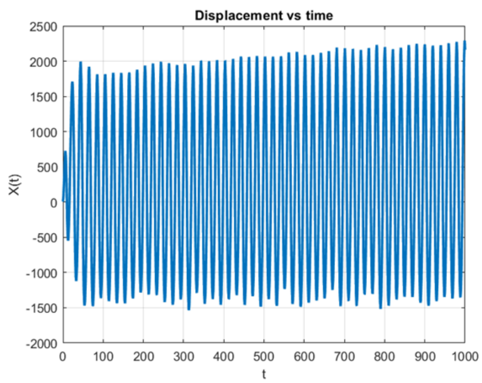

(a) Plot of Displacement vs. Time for k=1

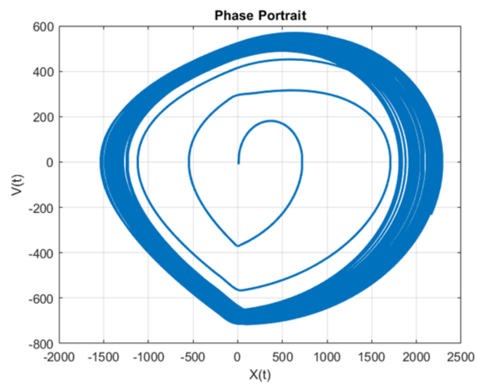

(b) Plot of Phase Portrait k=1

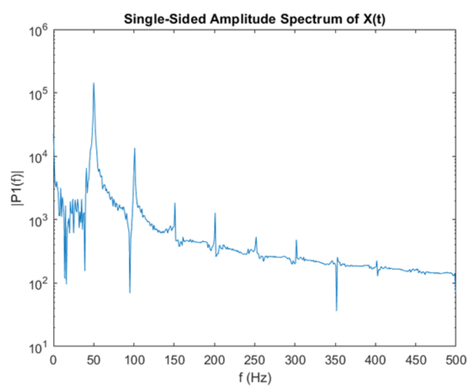

(c) Plot of Amplitude vs. Frequency for k=1

Figure 5.15: Analysis of System Dynamics: Displacement vs. Time, Amplitude vs. Frequency, and Phase Portrait for k=1

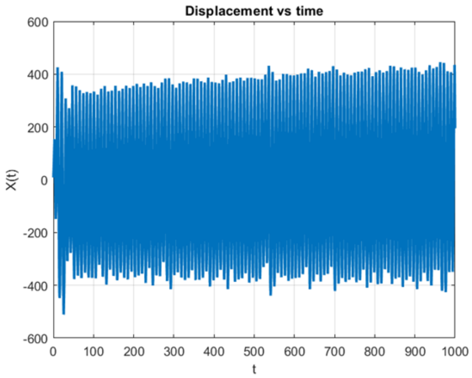

(a) Plot of Displacement vs. Time for k=5

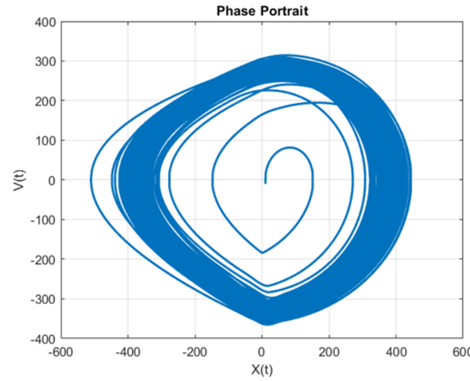

(b) Plot of Phase Portrait for k=5

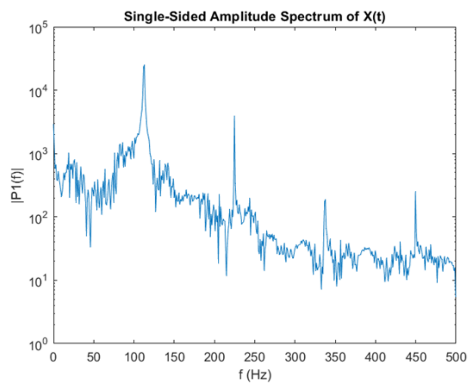

(c) Plot of Amplitude vs. Frequency for k=5

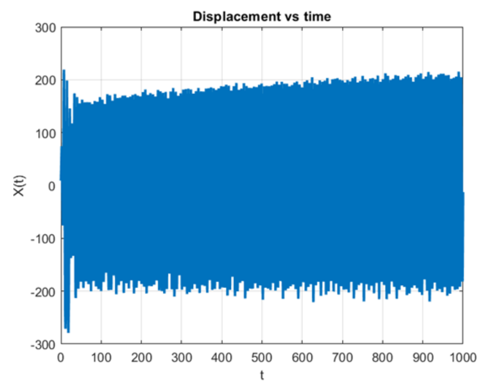

(d) Plot of Displacement vs. Time for k=10

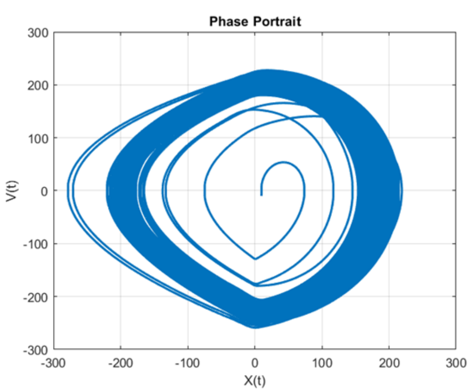

(e) Plot of Phase Portrait for k=10

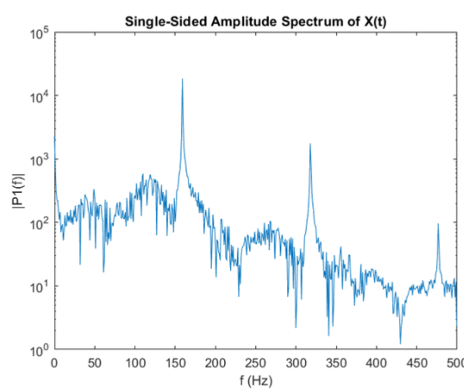

(f) Plot of Amplitude vs. Frequency for k=10

Figure 5.16: Analysis of System Dynamics for k=1 and k=5

5.2.6 Analysis of Nonlinear Vibration: Insights from Plots and Tables

Figures 5.4, 5.7, and 5.10 represent the plot of Displacement vs. Time for the case when mass is varying. Figures 5.5, 5.8, and 5.11 show the Phase Portrait for the same cases. Figures 5.6, 5.9, and 5.12 illustrate the Amplitude vs. Frequency plot for the varying mass cases.

Similarly, Figures 5.13a, 5.14a, and 5.14d represent the plot of Displacement vs. Time when the damping coefficient c is varying. Figures 5.13b, 5.14b, and 5.14e display the Phase Portraits, while Figures 5.13c, 5.14c, and 5.14f show the Amplitude vs. Frequency plots for varying c.

Finally, Figures 5.15a, 5.16a, and 5.16d depict the Displacement vs. Time plots for varying stiffness k. The corresponding Phase Portraits are shown in Figures 5.15b, 5.16b, and 5.16e, while the Amplitude vs. Frequency plots for varying k are presented in Figures 5.15c, 5.16c, and 5.16f.

5.2.7 Reasoning for Selection of External Force Components

There are two terms in external force component; The cosine term $100\cos\left(\sqrt{\frac{k}{m}}t\right)$ and $\sqrt{t}$ term. The cosine term $100\cos\left(\sqrt{\frac{k}{m}}t\right)$ was chosen to study the effect of periodic forces on the system. This periodic term vibrates at natural frequency of the system that is $\sqrt{k/m}$. By adding this term helps us to provide oscillations to the systems that helped in finding natural frequency of the system.

The term $\sqrt{t}$ was selected to introduce a non-linear, time-dependent aspect to the external force. It does not vary periodically and increases gradually over time. This term was chosen to make system more non linear so that we can increase the complexity of the system.

5.2.8 How Nonlinearity Excites Higher Harmonics

One important feature that characterises a system's reaction to external excitations is its single natural frequency, which is present in a single degree of freedom (SDOF) system. The system exhibits a predicted harmonic behaviour in a linear SDOF system. Higher harmonics are excited when nonlinearity is introduced into the system, which might drastically alter this response.

Higher harmonics are being excited in this study, as demonstrated above. This could be due to an external force acting on the system or to nonlinearity brought on by varying stiffness. Two figures are displayed here; 5.17 and 5.18 the first shows how stiffness varies, and the second illustrates how stiffness remains constant. There is an outside force in both system but variation of k causing excitation of higher harmonics in system.

The response of a linear system to a periodic excitation is usually restricted to the natural frequency and the external force frequency. But piecewise stiffness in this nonlinear SDOF system leads to sudden behaviour shifts and discontinuities, which in turn produce these higher harmonics. These harmonics reflect the greater dynamics of the nonlinear system by representing more intricate oscillation modes absent from a linear system.

Higher harmonics are a significant occurrence in nonlinear SDOF systems because they can impact the system's overall dynamics, such as stability, reactivity at various frequencies, and reaction to various external pressures.

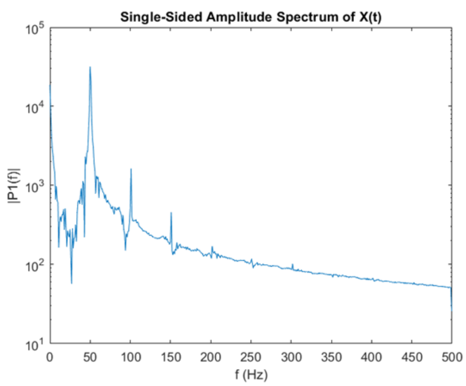

Figure 5.17: k is varying for +ve and -ve displacements

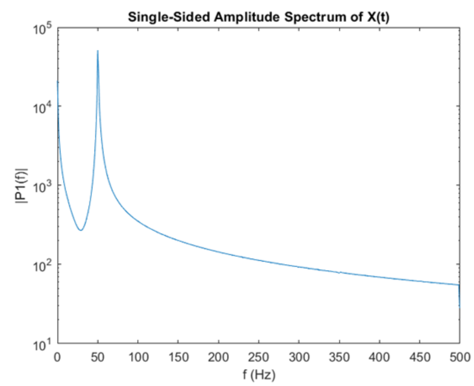

Figure 5.18: k is constant

In figures 5.17 and 5.18 it is shown even in the presence of external force in SDOF, it can't excites higher harmonics of system, but non linearity caused by stiffness can.

5.2.9 Challenges in Empirical Relation Determination

Attempts were made to derive an empirical relation between the system constants and the natural frequency. However, the non linear, complex and chaotic nature of the system and the randomness of the external force made it challenging to establish a clear empirical relationship.

Chapter 6

Free Vibration of membranes

6.1 Free Vibration of a Rectangular Membrane

6.1.1 Governing Equation

The governing partial differential equation (PDE) for the transverse displacement $w(x, y, t)$ of a rectangular membrane with unequal tension T_x and T_y is: [3]

$$\frac{\partial^2 w}{\partial t^2} = \frac{T_x}{\rho}\frac{\partial^2 w}{\partial x^2} + \frac{T_y}{\rho}\frac{\partial^2 w}{\partial y^2} \tag{6.1}$$

where ρ is the mass per unit area of the membrane.

6.1.2 Separation of Variables

Assume a solution of the form:

$$w(x, y, t) = X(x)Y(y)T(t) \tag{6.2}$$

Substitute this into the PDE:

$$X(x)Y(y)\frac{d^2T(t)}{dt^2} = \frac{T_x}{\rho}X''(x)Y(y)T(t) + \frac{T_y}{\rho}X(x)Y''(y)T(t) \tag{6.3}$$

Divide through by $X(x)Y(y)T(t)$ and rearrange:

$$\frac{1}{T(t)}\frac{d^2T(t)}{dt^2} = \frac{T_x}{\rho}\frac{X''(x)}{X(x)} + \frac{T_y}{\rho}\frac{Y''(y)}{Y(y)} \tag{6.4}$$

Let both sides equal a constant, $-\lambda^2$:

$$\frac{d^2T(t)}{dt^2} + \lambda^2 T(t) = 0 \tag{6.5}$$

$$\frac{T_x}{\rho}\frac{X''(x)}{X(x)} + \frac{T_y}{\rho}\frac{Y''(y)}{Y(y)} = -\lambda^2 \tag{6.6}$$

Separate into ordinary differential equations:

$$\frac{X''(x)}{X(x)} = -\lambda_x^2 \tag{6.7}$$

$$\frac{Y''(y)}{Y(y)} = -\lambda_y^2 \tag{6.8}$$

where:

$$\lambda^2 = \frac{T_x\lambda_y^2 + T_y\lambda_x^2}{\rho} \tag{6.9}$$

and:

$$\lambda_x^2 + \lambda_y^2 = \frac{\lambda^2\rho}{T_x} \tag{6.10}$$

6.1.3 Solutions for $X(x)$ and $Y(y)$

With boundary conditions $X(0) = X(a) = 0$ and $Y(0) = Y(b) = 0$, the solutions are:

$$X(x) = A\sin\left(\frac{n_x \pi x}{a}\right) \tag{6.11}$$

$$Y(y) = B\sin\left(\frac{n_y \pi y}{b}\right) \tag{6.12}$$

where n_x and n_y are positive integers.

6.1.4 Frequency Formula

Substitute these into the expression for λ^2:

$$\lambda^2 = \frac{\rho\pi^2}{a^2T_x}n_x^2 + \frac{\rho\pi^2}{b^2T_y}n_y^2 \tag{6.13}$$

The angular frequency ω is:

$$\omega = \lambda \sqrt{\frac{\rho}{T_x}} \tag{6.14}$$

Thus, the frequency f is:

$$f_{n_x,n_y} = \frac{1}{2\pi} \sqrt{\frac{\pi^2 \rho}{T_x} \left(\frac{n_x^2}{a^2} + \frac{T_x}{T_y} \frac{n_y^2}{b^2} \right)} \tag{6.15}$$

6.1.5 Numerical Solution Using Finite Difference Scheme

We employed the finite difference approach to solve the PDE numerically. Discrete differences are used in this method to approximate derivatives. This method involves discretising the domain into a number of grids for the membrane controlling PDE. It then generates algebraic equations by approximating the spatial derivatives, which may be solved using boundary conditions or a known value from the previous stage.

The analytical solution for four modes was compared with the numerical solution, which was calculated at different time steps.

6.1.6 Error Analysis

After obtaining the numerical results, the following steps were undertaken:

- **Comparison with Analytical Solution:** The numerical results produced in matlab were compared with the analytical solutions to compute accuracy.
- **Error Calculation:** The error between the numerical and analytical solutions was evaluated to see the performance of finite difference scheme.

The errors were calculated as:

$$\text{Error} = |\text{Numerical Solution} - \text{Analytical Solution}| \tag{6.16}$$

This process provides insight into the accuracy of the numerical method and its agreement with the analytical results.

6.1.7 Matlab plot of Various Modes of Vibration

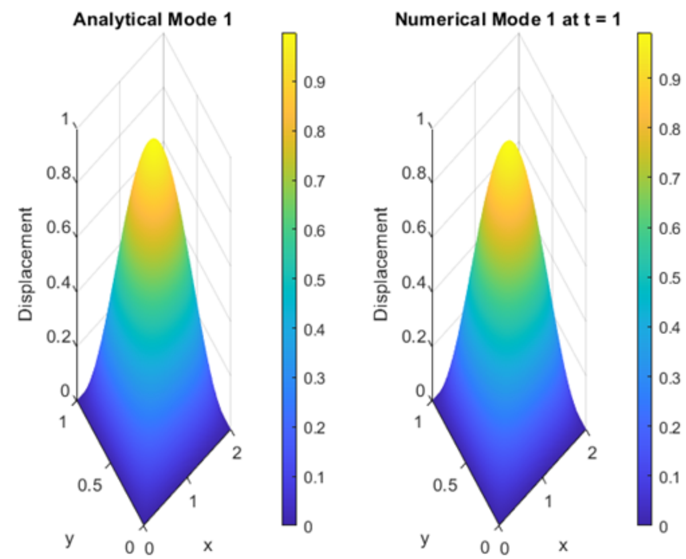

Figure 6.1: Comparison of Mode 1 Vibration for a Rectangular Membrane: Analytical Solution and Numerical Solution

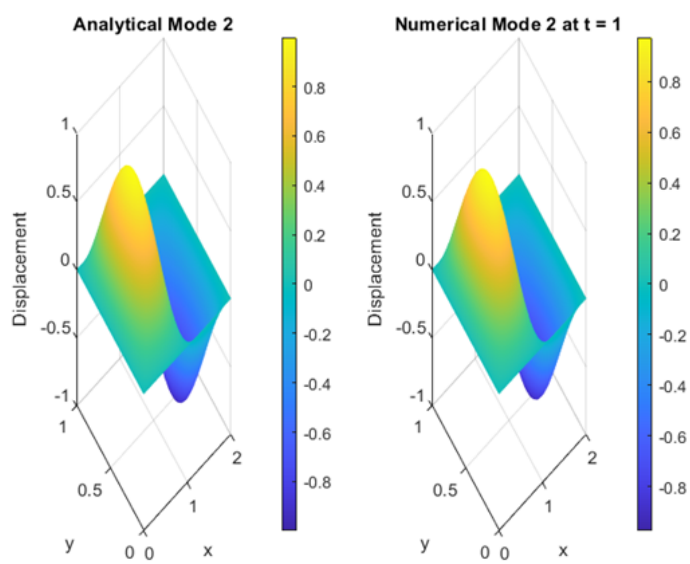

Figure 6.2: Comparison of Mode 2 Vibration for a Rectangular Membrane: Analytical Solution and Numerical Solution

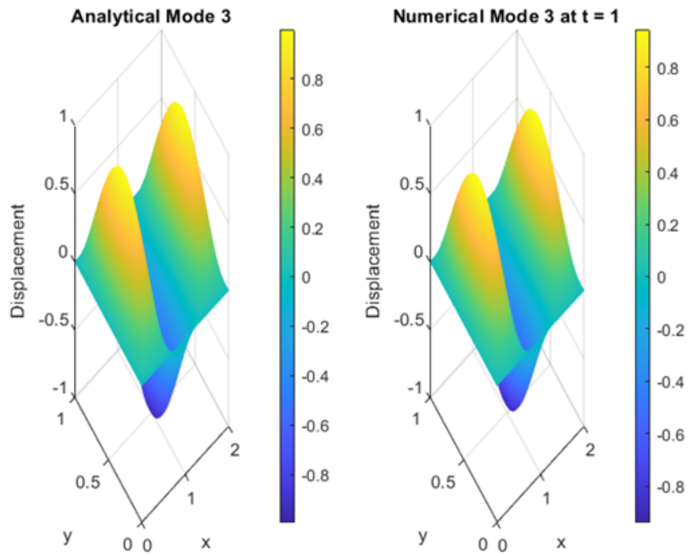

Figure 6.3: Comparison of Mode 3 Vibration for a Rectangular Membrane: Analytical Solution and Numerical Solution

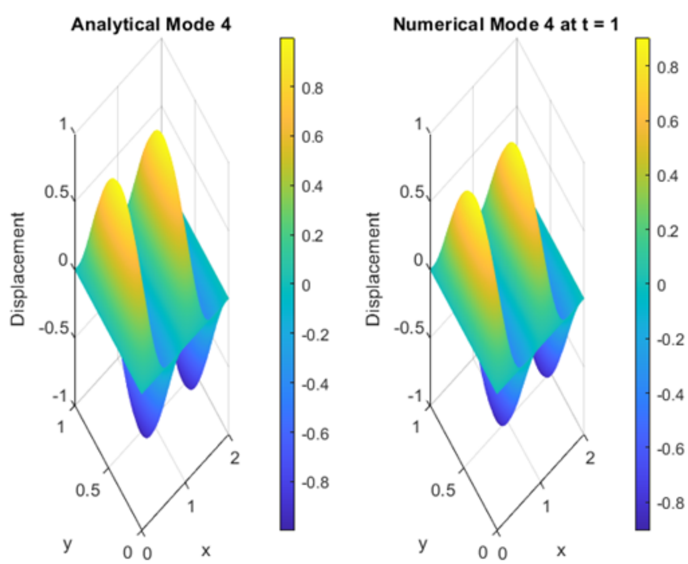

Figure 6.4: Comparison of Mode 4 Vibration for a Rectangular Membrane: Analytical Solution and Numerical Solution

6.1.8 Error and Frequency Table

Table 6.1: Mean Error for Different Modes for rectangular membrane

Mode	Mean Error
Mode 1	0.0027733
Mode 2	0.0098055
Mode 3	0.021214
Mode 4	0.036556

Table 6.2: Natural Frequencies of Different Modes for rectangular membrane

Mode	Natural Frequency 1
Mode 1	41.5594
Mode 2	49.6729
Mode 3	60.8367
Mode 4	73.6769

6.1.9 Conclusion

This work examined the free vibration of a rectangular membrane under uneven tension in the directions x and y. First, the method of variable separation was used to generate the analytical results from the governing partial differential equation. Analytical formulas for the mode shapes and natural frequencies are obtained from these results .

Numerical simulations employing a finite difference scheme were used to validate the analytical results. When the analytical answers and the numerical data were examined, there was good agreement across the various modes.6.1, 6.2, 6.3 and 6.4 represent plotting of analytical and numerical results in MATLAB for different modes. Each mode's errors were calculated to show how accurate the numerical approach used was.

Following the plotting of these analytical formulas for modes in Matlab, numerical results were obtained by utilising the finite difference scheme. The accuracy of the finite difference scheme was then confirmed by comparing the two outputs. Both the error and the natural frequency for each mode were computed as shown in table 6.1 and 6.2.

Overall, the work provides a thorough grasp of the dynamics involved in membrane vibrations and emphasises the significance of combining analytical and numerical methods to analyse membrane vibrations.

6.2 Free Vibration of a Circular Membrane

6.2.1 Governing Equation

The governing equation for the transverse displacement $w(r, \theta, t)$ of a circular membrane under unequal radial T_r and circumferential T_θ tensions is given by the two-dimensional wave equation: [3]

$$\frac{\partial^2 w}{\partial t^2} = \frac{T_r}{\rho}\left(\frac{\partial^2 w}{\partial r^2} + \frac{1}{r}\frac{\partial w}{\partial r}\right) + \frac{T_\theta}{\rho}\frac{1}{r^2}\frac{\partial^2 w}{\partial \theta^2} \tag{6.17}$$

where ρ is the mass per unit area of the membrane, r is the radial coordinate, and θ is the angular coordinate.

6.2.2 Separation of Variables

We assume a solution of the form:

$$w(r, \theta, t) = R(r)\Theta(\theta)T(t) \tag{6.18}$$

Substituting this into the governing equation and dividing by $R(r)\Theta(\theta)T(t)$ gives:

$$\frac{1}{T(t)}\frac{d^2T(t)}{dt^2} = \frac{T_r}{\rho}\left(\frac{R''(r)}{R(r)} + \frac{1}{r}\frac{R'(r)}{R(r)}\right) + \frac{T_\theta}{\rho}\frac{1}{r^2}\frac{\Theta''(\theta)}{\Theta(\theta)} \tag{6.19}$$

Let both sides equal a constant $-\lambda^2$, and separate the equation into two ordinary differential equations:

$$\frac{d^2T(t)}{dt^2} + \lambda^2 T(t) = 0 \tag{6.20}$$

$$\frac{T_\theta}{\rho}\frac{\Theta''(\theta)}{\Theta(\theta)} = -m^2 \tag{6.21}$$

$$\frac{T_r}{\rho}\left(r^2\frac{R''(r)}{R(r)} + r\frac{R'(r)}{R(r)}\right) + m^2 = -\lambda^2 r^2 \tag{6.22}$$

where m is an integer due to the periodic boundary conditions on θ.

6.2.3 Solution for $\Theta(\theta)$

The solution for the angular part is:

$$\Theta(\theta) = C\cos(m\theta) + D\sin(m\theta) \tag{6.23}$$

6.2.4 Solution for $R(r)$ Using Bessel Functions

The radial part of the equation can be expressed as:

$$r^2 R''(r) + rR'(r) + \left(\frac{\rho\lambda^2 r^2}{T_r} - m^2\right) R(r) = 0 \tag{6.24}$$

This is a Bessel's differential equation, and its solution is given by:

$$R(r) = J_m\left(\frac{\lambda r}{\sqrt{T_r/\rho}}\right) \tag{6.25}$$

where J_m is the Bessel function of the first kind of order m.

6.2.5 Frequency Formula

The boundary condition at $r = a$ (the membrane's radius) requires:

$$J_m\left(\frac{\lambda a}{\sqrt{T_r/\rho}}\right) = 0 \tag{6.26}$$

Let the n-th root of J_m be α_{mn}, then:

$$\frac{\lambda_{mn} a}{\sqrt{T_r/\rho}} = \alpha_{mn} \tag{6.27}$$

Thus, the angular frequency ω_{mn} is:

$$\omega_{mn} = \frac{\alpha_{mn}\sqrt{T_r/\rho}}{a} \tag{6.28}$$

The corresponding frequency f_{mn} is:

$$f_{mn} = \frac{\omega_{mn}}{2\pi} = \frac{\alpha_{mn}}{2\pi a}\sqrt{\frac{T_r}{\rho}} \tag{6.29}$$

By using this equation natural frequencies of the circular membrane can be expressed in terms of Bessel function zeros, membrane tension, mass per unit area, and radius.

6.2.6 MATLAB Implementation

Finite difference method was used to solve PDE numerically. This methods approximates derivatives using discrete differences. For the membrane governing PDE, this method involves discretising the domain into number of grids, use this method to generate algebraic equations by approximating the spatial derivatives and solve those equations using boundary conditions or known value at previous step.

The numerical solution was computed at various time steps, and the results were compared with the analytical solution for 4 modes. The resulting system of equations was solved at each time step to obtain the displacement $w(r, \theta, t)$ of the membrane at various grid points.

6.2.7 Error Analysis

After obtaining the numerical results, the following steps were undertaken:

- **Comparison with Analytical Solution:** The numerical results produced in matlab were compared with the analytical solutions to compute accuracy.
- **Error Calculation:** The error between the numerical and analytical solutions was evaluated to see the performance of finite difference scheme.

The errors were calculated as:

$$\text{Error} = |\text{Numerical Solution} - \text{Analytical Solution}| \tag{6.30}$$

This process provides insight into the accuracy of the numerical method and its agreement with the analytical results.

6.2.8 Matlab Plot of Various Modes of Vibration

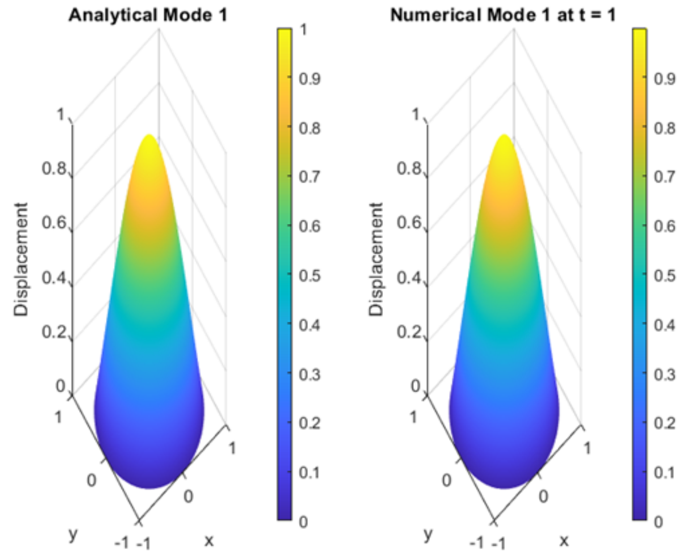

Figure 6.5: Comparison of Mode 1 Vibration for a Circular Membrane: Analytical Solution and Numerical Solution

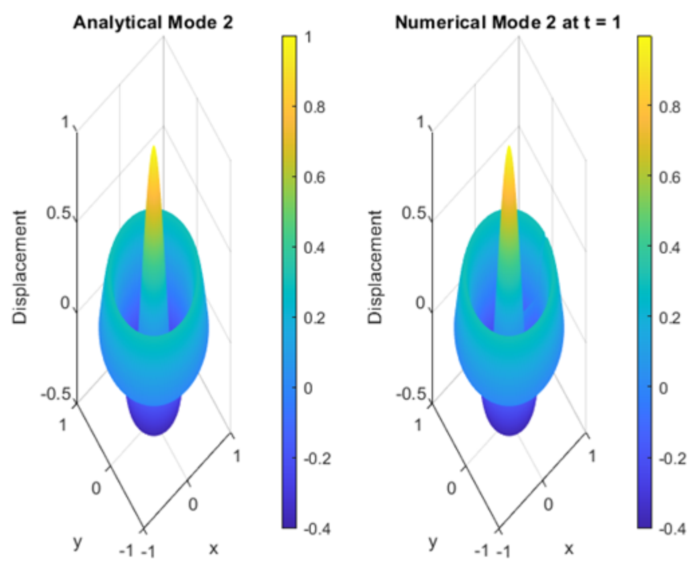

Figure 6.6: Comparison of Mode 2 Vibration for a Circular Membrane: Analytical Solution and Numerical Solution

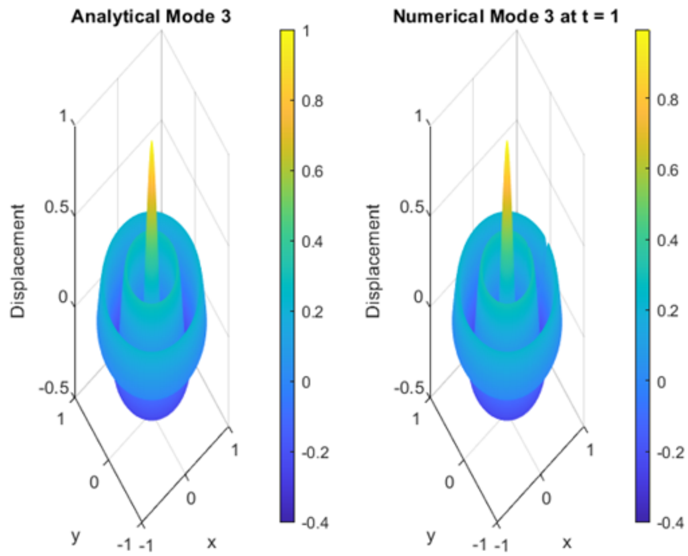

Figure 6.7: Comparison of Mode 3 Vibration for a Rectangular Membrane: Analytical Solution and Numerical Solution

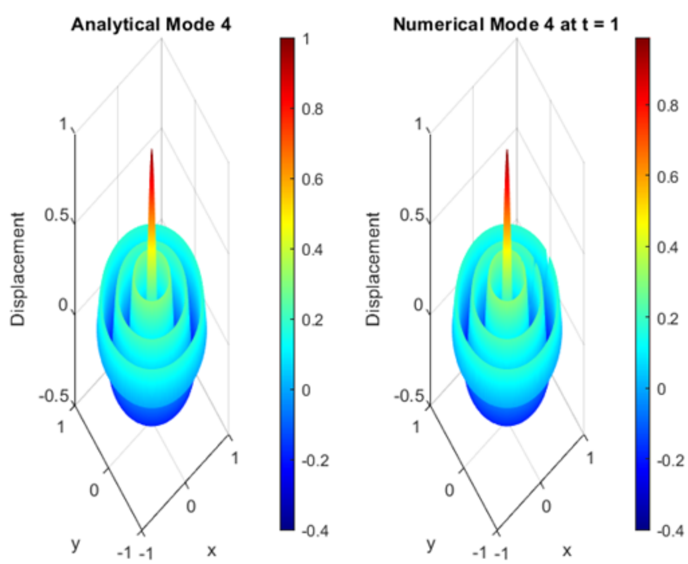

Figure 6.8: Comparison of Mode 4 Vibration for a Circular Membrane: Analytical Solution and Numerical Solution

6.2.9 Error and Frequency Table

Table 6.3: Mean Error for Different Modes for circular membrane

Mode	Mean Error
Mode 1	0.022005
Mode 2	0.016469
Mode 3	0.014947
Mode 4	0.014156

Table 6.4: Natural Frequencies of Different Modes for circular membrane

Mode	Natural Frequency
Mode 1	41.5594
Mode 2	49.6729
Mode 3	60.8367
Mode 4	73.6769

6.2.10 Conclusion

This work examined the free vibration of a circular membrane under uneven tension in the radial and circumferential directions. First, the method of variable separation leading to solutions in terms of Bessel functions was used to generate the analytical results from the governing partial differential equation. Analytical formulas for the mode shapes and natural frequencies are obtained from these results.

Numerical simulations employing a finite difference scheme were used to validate the analytical results. When the analytical answers and the numerical data were examined, there was good agreement across the various modes.6.5, 6.6, 6.7 and 6.8 represent plotting of analytical and numerical results in MATLAB for different modes. Each mode's errors were calculated to show how accurate the numerical approach used was.

Following the plotting of these analytical formulas for modes in Matlab, numerical results were obtained by utilising the finite difference scheme. The accuracy of the finite difference scheme was then confirmed by comparing the two outputs. Both the error and the natural frequency for each mode were computed as shown in table 6.3 and 6.4.

Overall, the work provides a thorough grasp of the dynamics involved in membrane vibrations and emphasises the significance of combining analytical and numerical methods to analyse membrane vibrations.

6.3 Free Vibration of an Elliptical Membrane

6.3.1 Governing Equation

The governing partial differential equation (PDE) for the transverse displacement $w(x, y, t)$ of an elliptical membrane with unequal tension T_x and T_y in the x and y directions, respectively, is given by: [3]

$$\frac{\partial^2 w}{\partial t^2} = \frac{T_x}{\rho}\frac{\partial^2 w}{\partial x^2} + \frac{T_y}{\rho}\frac{\partial^2 w}{\partial y^2} \tag{6.31}$$

where ρ is the mass per unit area of the membrane.

6.3.2 Separation of Variables

Assume a solution of the form:

$$w(x, y, t) = X(x)Y(y)T(t) \tag{6.32}$$

Substitute this into the PDE:

$$X(x)Y(y)\frac{d^2T(t)}{dt^2} = \frac{T_x}{\rho}X''(x)Y(y)T(t) + \frac{T_y}{\rho}X(x)Y''(y)T(t) \tag{6.33}$$

Divide through by $X(x)Y(y)T(t)$ and rearrange:

$$\frac{1}{T(t)}\frac{d^2T(t)}{dt^2} = \frac{T_x}{\rho}\frac{X''(x)}{X(x)} + \frac{T_y}{\rho}\frac{Y''(y)}{Y(y)} \tag{6.34}$$

Let both sides equal a constant, $-\lambda^2$:

$$\frac{d^2T(t)}{dt^2} + \lambda^2 T(t) = 0 \tag{6.35}$$

$$\frac{T_x}{\rho}\frac{X''(x)}{X(x)} + \frac{T_y}{\rho}\frac{Y''(y)}{Y(y)} = -\lambda^2 \tag{6.36}$$

Rearrange to obtain two separate ordinary differential equations:

$$\frac{X''(x)}{X(x)} = -\lambda_x^2 \tag{6.37}$$

$$\frac{Y''(y)}{Y(y)} = -\lambda_y^2 \tag{6.38}$$

where:

$$\lambda^2 = \frac{T_x \lambda_y^2 + T_y \lambda_x^2}{\rho} \tag{6.39}$$

and:

$$\lambda_x^2 + \lambda_y^2 = \frac{\lambda^2 \rho}{T_x} \tag{6.40}$$

6.3.3 Solution for $X(x)$ and $Y(y)$

The solutions $X(x)$ and $Y(y)$ are given in terms of Mathieu functions due to the elliptical geometry. For the x-direction, we solve:

$$\frac{d^2 X(x)}{dx^2} + \left(\lambda_x^2 - \frac{T_x}{\rho} \frac{T_y}{\rho} \frac{Y''(y)}{Y(y)} \right) X(x) = 0 \tag{6.41}$$

and for the y-direction:

$$\frac{d^2 Y(y)}{dy^2} + \left(\lambda_y^2 - \frac{T_y}{\rho} \frac{T_x}{\rho} \frac{X''(x)}{X(x)} \right) Y(y) = 0 \tag{6.42}$$

These equations are solved using Mathieu functions. The general solutions are:

$$X(x) = A\text{MathieuC}_n(\sqrt{\lambda_x^2} x) + B\text{MathieuS}_n(\sqrt{\lambda_x^2} x) \tag{6.43}$$

$$Y(y) = C\text{MathieuC}_m(\sqrt{\lambda_y^2} y) + D\text{MathieuS}_m(\sqrt{\lambda_y^2} y) \tag{6.44}$$

where MathieuC_n and MathieuS_n are the Mathieu cosine and sine functions, respectively, and n and m are the indices of these functions.

6.3.4 Frequency Formula

The angular frequency ω for the elliptical membrane is related to the Mathieu functions through the eigenvalues of these functions. The frequency formula is:

$$\omega_{mn} = \sqrt{\frac{T_x \lambda_{mn}^2 + T_y \lambda_{mn}^2}{\rho}} \tag{6.45}$$

where λ_{mn} are the eigenvalues associated with the Mathieu functions for the given mode indices m and n. The corresponding frequency f_{mn} is:

$$f_{mn} = \frac{\omega_{mn}}{2\pi} \tag{6.46}$$

Thus, the natural frequencies of the elliptical membrane are determined by the eigenvalues of the Mathieu functions and the membrane parameters (tensions T_x and T_y, mass per unit area ρ). The complete solution involves calculating these eigenvalues for specific mode shapes and then determining the corresponding frequencies.

6.3.5 Numerical Solution Using Finite Difference Scheme

Finite difference method was used to solve PDE numerically. This methods approximates derivatives using discrete differences. For the membrane governing PDE this method involves discretising the domain into number of grids, use this method to generate algebraic equations by approximating the spatial derivatives and solve those equations using boundary conditions or known value at previous step.

The numerical solution was computed at various time steps, and the results were compared with the analytical solution for 4 modes.

6.3.6 Comparison with Analytical Solution

The numerical results obtained from MATLAB were compared with the analytical solutions derived using Mathieu functions. For various vibration modes, the displacement profiles and natural frequencies were analyzed. The comparison aimed to validate the accuracy of the finite difference scheme and ensure that the numerical results align with theoretical expectations.

6.3.7 Error Calculation

To quantify the accuracy of the numerical solution, the error between the numerical results and the analytical solution was calculated. The error was computed at each grid point using the formula:

$$\text{Error}_{ij} = \left| w_{ij}^{\text{num}} - w_{ij}^{\text{ana}} \right| \tag{6.47}$$

where w_{ij}^{num} and w_{ij}^{ana} are the numerical and analytical displacements, respectively, at grid point (i, j). The mean error for each mode was obtained by averaging the errors over the entire domain:

$$
\text{Mean Error} = \frac{1}{N_x \times N_y} \sum_{i=1}^{N_x} \sum_{j=1}^{N_y} \text{Error}_{ij} \tag{6.48}
$$

This process provides insight into the accuracy of the numerical method and its agreement with the analytical results.

Table 6.5: Mean Error for Different Modes for elliptic membrane

Mode	Mean Error
Mode 1	0.49461
Mode 2	0.45056
Mode 3	0.45056
Mode 4	0.0

Table 6.6: Frequencies of different mode for elliptic membrane

Mode	Frequency
Mode 1	23
Mode 2	45
Mode 3	27
Mode 4	47

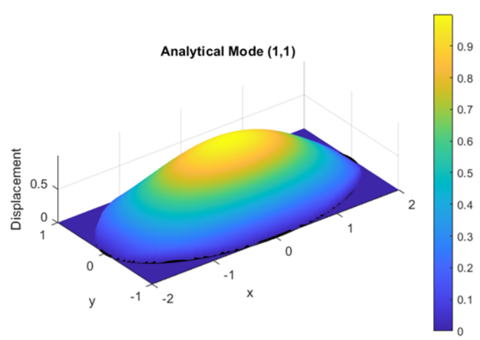

Figure 6.9: Analytical Vibration Mode 1 of the Elliptical Membrane

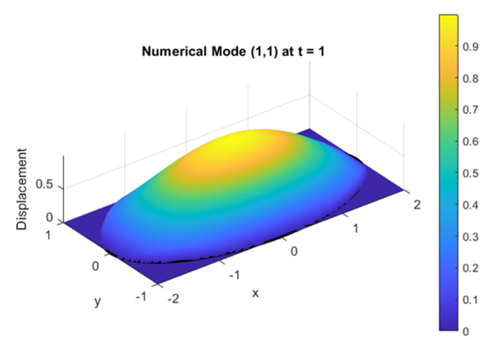

Figure 6.10: Numerical Vibration Mode 1 of the Elliptical Membrane

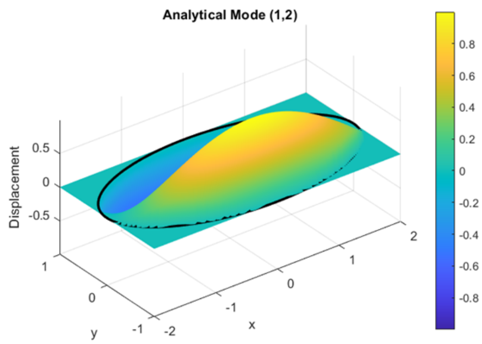

Figure 6.11: Analytical Vibration Mode 2 of the Elliptical Membrane

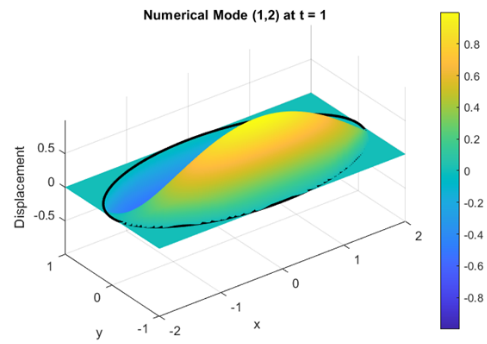

Figure 6.12: Numerical Vibration Mode 2 of the Elliptical Membrane

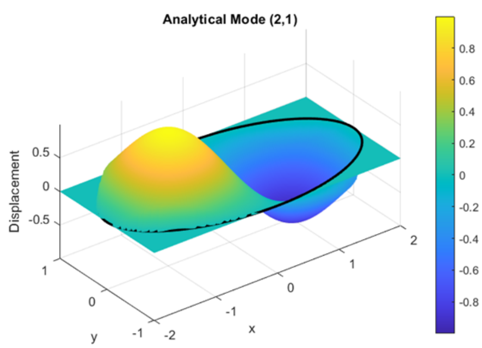

Figure 6.13: Analytical Vibration Mode 3 of the Elliptical Membrane

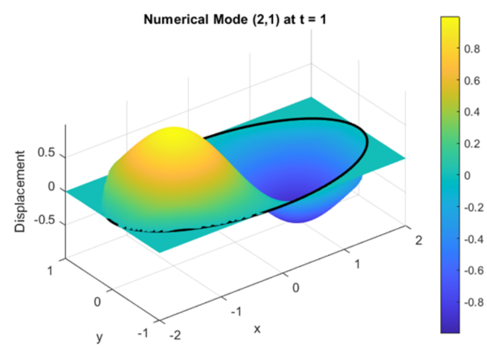

Figure 6.14: Numerical Vibration Mode 3 of the Elliptical Membrane

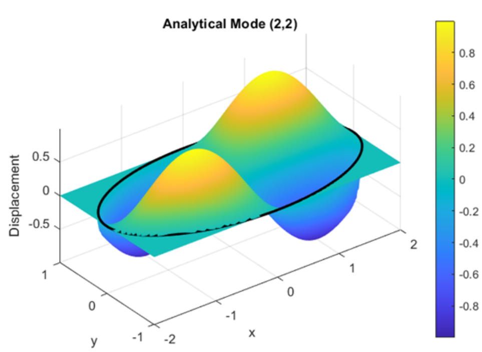

Figure 6.15: Analytical Vibration Mode 4 of the Elliptical Membrane

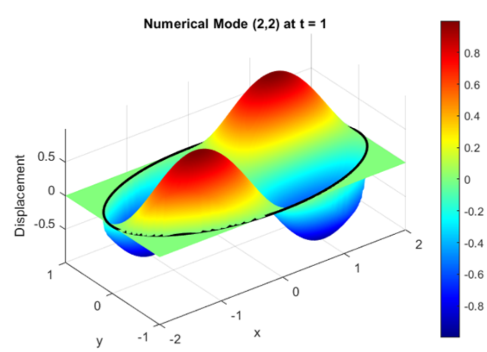

Figure 6.16: Numerical Vibration Mode 4 of the Elliptical Membrane

6.3.8 Conclusion

This work examined the free vibration of a elliptic membrane under uneven tension in the x and y directions. First, the method of variable separation leading to solutions in terms of Mathieu functions was used to generate the analytical results from the governing partial differential equation. Analytical formulas for the mode shapes and natural frequencies are obtained from these results.

Numerical simulations employing a finite difference scheme were used to validate the analytical results. When the analytical answers and the numerical data were examined, there was good agreement across the various modes.6.9, 6.11, 6.13 and 6.15 represent plotting of analytical results in MATLAB for different modes and 6.10, 6.12, 6.14 and 6.16 represent plotting of numerical results in MATLAB. Each mode's errors were calculated to show how accurate the numerical approach used was.

Following the plotting of these analytical formulas for modes in Matlab, numerical results were obtained by utilising the finite difference scheme. The accuracy of the finite difference scheme was then confirmed by comparing the two outputs. Both the error and the natural frequency for each mode were computed as shown in table 6.5 and 6.6.

Overall, the work provides a thorough grasp of the dynamics involved in membrane vibrations and emphasises the significance of combining analytical and numerical methods to analyse membrane vibrations.

Chapter 7

Non linear vibration of membrane

7.1 Analytical derivations of nonlinear vibration of membrane

When vibration amplitude of the membrane is much larger than its thickness, in that case influence of damping cannot be neglected. This is why we are focusing on these aspects in this study.

7.1.1 Structural Model

Consider a rectangular orthotropic membrane with its edges fixed. The two orthogonal directions x and y are the principal fiber directions. The lengths in these directions are denoted by a and b, respectively. The initial tensions in the x and y directions are N_{0x} and N_{0y}, respectively. The impact loading is caused by a pellet, which can be considered as a particle with an initial velocity v_0 and mass M. The impact contact point is located at (x_0, y_0).

7.1.2 Impact Load Expression

The impact load on the membrane can be expressed as:

$$p(x, y, t) = F(t)\delta(x - x_0)\delta(y - y_0) \tag{7.1}$$

where $p(x, y, t)$ is the impact load, $F(t)$ is the time-dependent impact force, and δ denotes the Dirac delta function. [2]

7.1.3 Initial Conditions

- **Initial Displacement:**

$$w(x_0, y_0, t)\big|_{t=0} = 0 \tag{7.2}$$

- **Initial Velocity:**

$$\frac{\partial w(x_0, y_0, t)}{\partial t}\Big|_{t=0} = v_0 \tag{7.3}$$

  where v_0 is the initial velocity at $t = 0$. [2]

7.1.4 Impulse-Momentum Relation

The impulse-momentum relation is given by: [2]

$$\int_0^t F(\tau)\, d\tau = Mv_0 - M\frac{\partial w(x_0, y_0, t)}{\partial t}\Big|_{t=0}. \tag{7.4}$$

7.1.5 Differentiation with Respect to Time

Differentiate 7.4 with respect to time t: [2]

$$\frac{d}{dt}\left(\int_0^t F(\tau)\, d\tau\right) = \frac{d}{dt}\left(Mv_0 - M\frac{\partial w(x_0, y_0, t)}{\partial t}\Big|_{t=0}\right) \tag{7.5}$$

The left side simplifies to $F(t)$:

$$F(t) = \frac{d}{dt}\left(\int_0^t F(\tau)\, d\tau\right) \tag{7.6}$$

The right side simplifies to:

$$\frac{d}{dt}(Mv_0) - \frac{d}{dt}\left(M\frac{\partial w(x_0, y_0, t)}{\partial t}\Big|_{t=0}\right) \tag{7.7}$$

Since Mv_0 is constant with respect to t, its derivative is zero:

$$F(t) = -M\frac{\partial^2 w(x_0, y_0, t)}{\partial t^2} \tag{7.8}$$

7.1.6 Damped Forced Vibration Partial Differential Motion Equation

According to the Von Kármán large deflection theory and D'Alembert's principle, the damped forced vibration partial differential motion equation for an orthotropic membrane is given by:

$$\rho\frac{\partial^2 w}{\partial t^2} + c\frac{\partial w}{\partial t} - (N_x + N_{0x})\frac{\partial^2 w}{\partial x^2} - (N_y + N_{0y})\frac{\partial^2 w}{\partial y^2} = p(x, y, t) \tag{7.9}$$

where:

- ρ is the aerial density of the membrane.
- c is the viscous damping coefficient.
- N_x and N_y are additional tensions in the x and y directions, respectively.
- N_{0x} and N_{0y} are initial tensions in the x and y directions, respectively.
- $p(x, y, t)$ is the impact loading. [2]

7.1.7 Consistency Equation

The consistency equation is:

$$\frac{1}{E_1 h}\frac{\partial^2 N_x}{\partial y^2} - \frac{\mu_2}{E_2 h}\frac{\partial^2 N_y}{\partial y^2} - \frac{\mu_1}{E_1 h}\frac{\partial^2 N_x}{\partial x^2} + \frac{1}{E_1 h}\frac{\partial^2 N_y}{\partial x^2} = \left(\frac{\partial^2 w}{\partial x \partial y}\right)^2 - \frac{\partial^2 w}{\partial x^2}\frac{\partial^2 w}{\partial y^2} \tag{7.10}$$

where:

- E_1 and E_2 are Young's moduli in the x and y directions, respectively.
- μ_1 and μ_2 are Poisson's ratios in the x and y directions, respectively.
- N_x and N_y are additional tensions in the x and y directions, respectively.
- h is the thickness of the membrane. [2]

7.1.7.1 Stress Functions

The stress functions are given by: [2]

$$N_x = h\frac{\partial^2 \varphi}{\partial y^2} \tag{7.11}$$

$$N_{0x} = h\sigma_{0x} \tag{7.12}$$

$$N_y = h\frac{\partial^2 \varphi}{\partial x^2} \tag{7.13}$$

$$N_{0y} = h\sigma_{0y} \tag{7.14}$$

7.1.7.2 Substituting Stress Functions

Substitute 7.11, 7.12, 7.13 and7.14 into the equation 7.9 yields : [2]

$$\rho\frac{\partial^2 w}{\partial t^2} + c\frac{\partial w}{\partial t} - \left(h\frac{\partial^2 \varphi}{\partial y^2} + h\sigma_{0x}\right)\frac{\partial^2 w}{\partial x^2} - \left(h\frac{\partial^2 \varphi}{\partial x^2} + h\sigma_{0y}\right)\frac{\partial^2 w}{\partial y^2} = p(x, y, t) \tag{7.15}$$

Simplify the equation:

$$\rho\frac{\partial^2 w}{\partial t^2} + c\frac{\partial w}{\partial t} - h\frac{\partial^2 \varphi}{\partial y^2}\frac{\partial^2 w}{\partial x^2} - h\sigma_{0x}\frac{\partial^2 w}{\partial x^2} - h\frac{\partial^2 \varphi}{\partial x^2}\frac{\partial^2 w}{\partial y^2} - h\sigma_{0y}\frac{\partial^2 w}{\partial y^2} = p(x, y, t) \tag{7.16}$$

7.1.8 Consistency Equation

Substitute 7.11 and 7.13 into the equation 7.10 and simplifying the equation:

$$\frac{1}{E_1}\frac{\partial^4 \varphi}{\partial y^4} + \frac{1}{E_2}\frac{\partial^4 \varphi}{\partial x^4} = \left(\frac{\partial^2 w}{\partial x \partial y}\right)^2 - \frac{\partial^2 w}{\partial x^2}\frac{\partial^2 w}{\partial y^2} \tag{7.17}$$

where:

- φ is the stress function.
- E_1 and E_2 are Young's moduli in the y and x directions, respectively.
- w is the deflection of the membrane. [2]

7.1.9 Boundary Conditions

7.1.9.1 Boundary Conditions for Displacement $w(x, y, t)$

At $x = 0$ and $x = a$ (Boundaries in the x-direction): [2]

$$w(0, y, t) = 0 \tag{7.18}$$

$$\frac{\partial^2 w}{\partial x^2}(0, y, t) = 0 \tag{7.19}$$

$$w(a, y, t) = 0 \tag{7.20}$$

$$\frac{\partial^2 w}{\partial x^2}(a, y, t) = 0 \tag{7.21}$$

At $y = 0$ and $y = b$ (Boundaries in the y-direction):

$$w(x, 0, t) = 0 \tag{7.22}$$

$$\frac{\partial^2 w}{\partial y^2}(x, 0, t) = 0 \tag{7.23}$$

$$w(x, b, t) = 0 \tag{7.24}$$

$$\frac{\partial^2 w}{\partial y^2}(x, b, t) = 0 \tag{7.25}$$

7.1.9.2 Boundary Conditions for Stress Function $\varphi(x, y, t)$

At $x = 0$ and $x = a$: [2]

$$\frac{\partial^2 \varphi}{\partial x^2}(0, y, t) = 0 \tag{7.26}$$

$$\frac{\partial^2 \varphi}{\partial x^2}(a, y, t) = 0 \tag{7.27}$$

At $y = 0$ and $y = b$:

$$\frac{\partial^2 \varphi}{\partial y^2}(x, 0, t) = 0 \tag{7.28}$$

$$\frac{\partial^2 \varphi}{\partial y^2}(x, b, t) = 0 \tag{7.29}$$

7.1.10 Functions Satisfying Boundary Conditions

7.1.10.1 Displacement Function $w(x, y, t)$

The displacement function is given by:

$$w(x, y, t) = \sum_{m=1}^{\infty} \sum_{n=1}^{\infty} T_{mn}(t) W_{mn}(x, y) \tag{7.30}$$

where the mode shape function $W_{mn}(x, y)$ is:

$$W_{mn}(x, y) = \sin\left(\frac{m\pi x}{a}\right) \sin\left(\frac{n\pi y}{b}\right) \tag{7.31}$$

The function $W_{mn}(x, y)$ automatically satisfies the displacement boundary conditions. [2]

7.1.10.2 Stress Function $\varphi(x, y, t)$

The stress function is given by:

$$\varphi(x, y, t) = \sum_{m=1}^{\infty} \sum_{n=1}^{\infty} T_{mn}^2(t) \phi_{mn}(x, y) \tag{7.32}$$

where $\phi_{mn}(x, y)$ is the mode shape function for the stress function. This function $\phi_{mn}(x, y)$ should be defined to satisfy the stress boundary conditions. [2]

7.1.10.3 Simplified Notation

To simplify the notation: [2]

- Let $W(x, y) = W_{mn}(x, y)$ and $\varphi(x, y) = \varphi_{mn}(x, y)$.
- Let $T(t) = T_{mn}(t)$ for the time-dependent function.

Thus, the simplified expressions are:
Displacement Function:

$$w(x, y, t) = T(t) W(x, y) \tag{7.33}$$

where

$$W(x, y) = \sin\left(\frac{m\pi x}{a}\right) \sin\left(\frac{n\pi y}{b}\right) \tag{7.34}$$

Stress Function:

$$\varphi(x,y,t) = \sum_{m=1}^{\infty}\sum_{n=1}^{\infty} T_{mn}^{2}(t)\phi_{mn}(x,y) \tag{7.35}$$

7.1.11 Stress Function

By substituting equation 7.33, 7.34 and 7.35 in equation 7.17 we get: [2]

$$\frac{1}{E_1}\frac{\partial^4\phi}{\partial y^4} + \frac{1}{E_2}\frac{\partial^4\phi}{\partial x^4} = \frac{m^2n^2\pi^4}{2a^2b^2}\left(\cos\left(\frac{2m\pi x}{a}\right) + \cos\left(\frac{2n\pi y}{b}\right)\right) \tag{7.36}$$

Assume the solution of the equation 7.36 is given by:

$$\phi(x,y) = \alpha\cos\left(\frac{2m\pi x}{a}\right) + \beta\cos\left(\frac{2n\pi y}{b}\right) + \gamma_1x^3 + \gamma_2x^2 + \gamma_3y^3 + \gamma_4y^2 \tag{7.37}$$

where:

- α and β are coefficients for the cosine terms,
- γ_1 and γ_3 are coefficients for x^3 and y^3,
- γ_2 and γ_4 are coefficients for x^2 and y^2.

Substitute above solution into equation we get:

$$\alpha = \frac{32m^2b^2}{E_2n^2a^2} \tag{7.38}$$

$$\beta = \frac{32n^2a^2}{E_1m^2b^2} \tag{7.39}$$

7.1.12 Boundary Conditions and Constants

From the boundary conditions: [2]

$$\gamma_1 = \gamma_3 = 0 \tag{7.40}$$

$$\gamma_2 = \frac{16b^2}{E_2n^2\pi^2} \tag{7.41}$$

$$\gamma_4 = \frac{16a^2}{E_1m^2\pi^2} \tag{7.42}$$

7.1.13 Final Differential Equation

By substituting displacement function w and stress function φ into Damped Forced Vibration Partial Differential Motion Equation and Using the Bubnov-Galerkin method, the final differential equation is:

$$\frac{d^2T(t)}{dt^2}+\frac{c}{\rho}\frac{dT(t)}{dt}+\frac{m^2\pi^2b^2N_{0x}+n^2\pi^2a^2N_{0y}}{\rho a^2b^2}T(t)+\frac{2m^2n^2\pi^4\beta+2m^2n^2\pi^4\alpha\frac{a^2}{b^2}\rho T^3(t)}{a^2b^2\rho}=\frac{4F(t)}{ab\rho}\times P \tag{7.43}$$

where P=

$$\sin\left(\frac{m\pi x_0}{a}\right)\sin\left(\frac{n\pi y_0}{b}\right)$$

Given the expression for $F(t)$:

$$F(t)=-M\frac{\partial^2 w(x_0,y_0,t)}{\partial t^2} \tag{7.44}$$

Substitute equation 7.44 into 7.43 results in:

$$\frac{d^2T(t)}{dt^2}+\frac{ca^2b^2}{\rho a^2b^2+4abM\sin^2\left(\frac{m\pi x_0}{a}\right)\sin^2\left(\frac{n\pi y_0}{b}\right)}\frac{dT(t)}{dt}+A\times T(t)+B\times T^3(t)=0 \tag{7.45}$$

where A=

$$\frac{m^2\pi^2b^2N_{0x}+n^2\pi^2a^2N_{0y}}{\rho a^2b^2+4abM\sin^2\left(\frac{m\pi x_0}{a}\right)\sin^2\left(\frac{n\pi y_0}{b}\right)}$$

and B=

$$\frac{2m^2n^2\pi^4h\beta+2m^2n^2\pi^4h\alpha}{\rho a^2b^2+4abM\sin^2\left(\frac{m\pi x_0}{a}\right)\sin^2\left(\frac{n\pi y_0}{b}\right)}$$

Equation 7.45 is a nonlinear with respect to T(t). Due to the presence of a damping term, the solution to Equation will not be periodic. Furthermore, since Equation 7.45 is nonlinear, finding an accurate analytical solution is quite challenging. KBM perturbation method has been used to obtain the approximate analytical solution that satisfies above nonlinear diffrential equation.

Assume that the perturbation parameter is $\epsilon=\left(\frac{h^2}{ab}\right)^{-1}$ and by letting $y=T(t)$, Above non linear equation can be simplified as:

$$\ddot{y}+\omega_0^2y=\epsilon\left(\alpha_1y^3+\alpha_2\dot{y}\right) \tag{7.46}$$

where

$$\omega_0^2 = \frac{m^2\pi^2 b^2 N_{0x} + n^2\pi^2 a^2 N_{0y}}{\rho a^2 b^2 + 4abM \sin^2\left(\frac{m\pi x_0}{a}\right)\sin^2\left(\frac{n\pi y_0}{b}\right)} \tag{7.47}$$

Expression for α_1:

$$\alpha_1 = \frac{-2m^2n^2\pi^4(\alpha+\beta)}{h\rho ab + 4M \sin^2\left(\frac{m\pi x_0}{a}\right)\sin^2\left(\frac{n\pi y_0}{b}\right)} \tag{7.48}$$

Expression for α_2:

$$\alpha_2 = \frac{-ca^2b^2}{h^2\rho ab + 4M \sin^2\left(\frac{m\pi x_0}{a}\right)\sin^2\left(\frac{n\pi y_0}{b}\right)} \tag{7.49}$$

According to the KBM perturbation method, let $f(y, \dot{y}) = (\alpha_1 y^3 + \alpha_2 \dot{y})$ and the solution of above equation is:

$$y = a\cos(\phi) \tag{7.50}$$

In Equation 7.50, a and ϕ are determined by using the following equations:

$$\frac{da}{dt} = -\frac{\epsilon\omega_0 A_0(a)}{dt} \tag{7.51}$$

$$\frac{d\phi}{dt} = \omega_0 - \frac{\epsilon\omega_0 C_0(a)}{dt} \tag{7.52}$$

Calculation of $A_0(a)$:

The term $A_0(a)$ is computed from the integral involving $\sin\phi$:

$$A_0(a) = \frac{1}{2}\int_0^{2\pi} \sin\left(f(a\cos\phi - a\omega_0\sin\phi)\right) d\phi \tag{7.53}$$

$$A_0(a) = -\frac{1}{2}\alpha_2 a\omega_0 \tag{7.54}$$

Calculation of $C_0(a)$:

The term $C_0(a)$ is computed from the integral involving $\cos\phi$:

$$C_0(a) = \frac{1}{2}\int_0^{2\pi} \cos\left(f(a\cos\phi - a\omega_0\sin\phi)\right) d\phi \tag{7.55}$$

$$C_0(a) = \frac{3}{8}\alpha_1 a^3 \tag{7.56}$$

Thus, the equations for a and φ become:

Differential Equations

$$\frac{da}{dt} = \frac{\epsilon\alpha_2}{2}a \tag{7.57}$$

$$\frac{d\varphi}{dt} = \omega_0 - \frac{3\epsilon\alpha_1 a^2}{8\omega_0} \tag{7.58}$$

Integrated Solutions

$$a(t) = De^{0.5\alpha_2\epsilon t} \tag{7.59}$$

$$\varphi(t) = \left(\omega_0 - \frac{3\alpha_1 a^2\epsilon}{8\omega_0}\right)t + \varphi_0 \tag{7.60}$$

By substituting 7.59 and 7.60 back into the 7.50, we get:

Final Solution for $y(t)$

$$y(t) = De^{0.5\alpha_2\epsilon t}\cos\left(\left(\omega_0 - \frac{3\alpha_1 D^2\epsilon e^{\alpha_2\epsilon t}}{8\omega_0}\right)t + \varphi_0\right) \tag{7.61}$$

The frequency of the nonlinear damped forced vibration of a pre-stressed orthotropic membrane structure is given by :

$$\omega_{\text{nonlinear}} = \left(\omega_0 - \frac{3\alpha_1 D^2\epsilon e^{\alpha_2\epsilon t}}{8\omega_0}\right) \tag{7.62}$$

This expression represents the time-dependent frequency of the system. The natural frequency ω_0 is governed by the nonlinear term $\frac{3\alpha_1 D^2\epsilon e^{\alpha_2\epsilon t}}{8\omega_0}$, which depends on the amplitude D, damping ϵ, the parameters α_1, α_2, and the time t. We use the initial conditions to determine D and φ_0. The impact actuation duration for the pellet impacting the membrane is very short, so the system formed by the pellet and membrane can be considered a conservative system. According to the principle of conservation of momentum, we can obtain the following expression:

$$Mv_0 = Mv_0' + \iint_S v_0' W(x,y)\, ds \tag{7.63}$$

where $W(x,y)$ is the initial deformation function, v_0 is the initial velocity of the pellet, and v_0' is the initial velocity of the pellet and the impact point of the membrane after impact. The initial deformation of the membrane is assumed as:

$$W(x,y) = \sin\left(\frac{\pi x}{a}\right)\sin\left(\frac{\pi y}{b}\right) \tag{7.64}$$

The substitution of equation 7.64 into the equation 7.63 yields:

$$v_0' = \frac{M v_0}{M + \frac{4\rho ab}{\pi^2}} \tag{7.65}$$

The pellet and membrane have the same initial velocity v_0' at the time $t = 0$. We can therefore obtain the following initial condition:

$$\left.\frac{\partial w(x_0, y_0, t)}{\partial t}\right|_{t=0} = \sin\left(\frac{m\pi x_0}{a}\right)\sin\left(\frac{n\pi y_0}{b}\right)\left.\frac{dT(t)}{dt}\right|_{t=0} = v_0' \tag{7.66}$$

i.e.,

$$\left.\frac{dy(t)}{dt}\right|_{t=0} = \left.\frac{dT(t)}{dt}\right|_{t=0} = \frac{v_0'}{\sin\left(\frac{m\pi x_0}{a}\right)\sin\left(\frac{n\pi y_0}{b}\right)} \tag{7.67}$$

Another initial condition is that the initial displacement of the impact point on the membrane is zero at the time $t = 0$. We can obtain the following initial condition:

$$\left.w(x_0, y_0, t)\right|_{t=0} = \sin\left(\frac{m\pi x_0}{a}\right)\sin\left(\frac{n\pi y_0}{b}\right)\left.T(t)\right|_{t=0} = 0 \tag{7.68}$$

i.e.,

$$\left.y(t)\right|_{t=0} = \left.T(t)\right|_{t=0} = 0 \tag{7.69}$$

The substitution of equation 7.61 into equation 7.69:

$$0 = D\cos(\varphi_0) \tag{7.70}$$

In this equation, $D \neq 0$, so there must be $\cos(\varphi_0) = 0$. Then $\varphi_0 = \frac{\pi}{2} + k\pi$ (where $k = 1, 3, 5, 7, \ldots$). We can take $\varphi_0 = \frac{\pi}{2}$, and by substituting it into the original equation and performing the differentiation, one obtains:

$$\frac{dy(t)}{dt} = \frac{1}{2}D\alpha_2\epsilon e^{0.5\alpha_2\epsilon t}\cos\left[\left(\omega_0 - \frac{3\alpha_1\epsilon D^2 e^{\alpha_2\epsilon t}}{8\omega_0}\right)t + \frac{\pi}{2}\right] - De^{0.5\alpha_2\epsilon t}\sin\left[\left(\omega_0 - \frac{3\alpha_1\epsilon D^2 e^{\alpha_2\epsilon t}}{8\omega_0}\right)t + \frac{\pi}{2}\right]$$
$$\left(\omega_0 - \frac{3\alpha_1\epsilon D^2 e^{\alpha_2\epsilon t}}{8\omega_0} - (\frac{3\alpha_1\alpha_2\epsilon^2 D^2 e^{\alpha_2\epsilon t}}{8\omega_0})t\right) \tag{7.71}$$

where the frequency of the nonlinear damped forced vibration of the pre-stressed orthotropic membrane structure is the term inside the cosine function, multiplied by t. The frequency depends on the amplitude and damping.

Substitution of equation 7.71 into equation

$$\left.\frac{dy(t)}{dt}\right|_{t=0} = \left.\frac{dT(t)}{dt}\right|_{t=0} = \frac{v_0'}{\sin\left(\frac{m\pi x_0}{a}\right)\sin\left(\frac{n\pi y_0}{b}\right)} \tag{7.72}$$

yields:

$$D\left(\frac{3\alpha_1 D^2\epsilon}{8\omega_0} - \omega_0\right) = v_0'\sin\left(\frac{m\pi x_0}{a}\right)\sin\left(\frac{n\pi y_0}{b}\right) \tag{7.73}$$

By solving above equation, we can obtain the expression for the amplitude D. There are three roots. Two roots are complex and one root is real. The amplitude D is real, and so the expression for D is given by:

$$\text{numerator} = \sqrt{81\epsilon^4 {v_0}^2\alpha_1^4\omega_0^2\left(\frac{1}{\sin^2\left(\frac{m\pi x_0}{a}\right)}\right)\left(\frac{1}{\sin^2\left(\frac{n\pi y_0}{b}\right)}\right) - 32\epsilon^3\alpha_1^3\omega_0^6}$$

$$\text{denominator} = 3\epsilon\alpha_1$$

$$D = \frac{-4\cdot 2^{1/3}\cdot\omega_0^2}{3\cdot\left(\text{numerator} - 9\epsilon^2 v_0\alpha_1^2\omega_0\cdot\frac{1}{\sin\left(\frac{m\pi x_0}{a}\right)}\cdot\frac{1}{\sin\left(\frac{n\pi y_0}{b}\right)}\right)^{1/3}} - \frac{2^{2/3}\cdot\left(\text{numerator} - 9\epsilon^2 v_0\alpha_1^2\omega_0\cdot\frac{1}{\sin\left(\frac{m\pi x_0}{a}\right)}\cdot\frac{1}{\sin\left(\frac{n\pi y_0}{b}\right)}\right)^{1/3}}{3\epsilon\alpha_1}$$

By substituting equation 7.61 into Equation 7.30 we can obtain the displacement expression:

$$w(x,y,t) = \sum_{m=1}^{\infty}\sum_{n=1}^{\infty}\sin\left(\frac{m\pi x}{a}\right)\sin\left(\frac{n\pi y}{b}\right)De^{0.5\epsilon t}\cos\left(\left(\omega_0 - \frac{3\alpha_1 D^2\epsilon e^{\alpha_2\epsilon t}}{8\omega_0}\right)t + \pi/2\right)] \tag{7.74}$$

By taking the first derivative and second derivative of Equation 7.74 , we can obtain the velocity and acceleration expressions. According to Equation 7.74, we can obtain the lateral displacement of any point on the membrane surface, and analyze the vibration modes and displacement time histories of each point on the membrane surface. [2]

7.1.14 Analytical Solutions for Different Modes

Analytical solutions for different modes of the membrane were derived as mentioned in report. These analytical solutions were plotted in MATLAB to visualize the behavior of the membrane under each mode. These plot 7.1, 7.2, 7.3 and 7.4, provides understanding about distinct characteristics and patterns associated with each mode of vibration.

7.1.15 Amplitude vs. Time Analysis

After that, amplitude vs time graph was also plotted in MATLAB shown in figure 7.5 and 7.6, to reveal how oscillations of membrane proceeds with time. This analysis provided deep insight about dynamic response of the system and the factors influencing the amplitude of vibration.

7.1.16 Frequency vs. Time Analysis

Analytical solutions for frequency dependence on time were derived as mentioned in paper. This expression represents the time-dependent frequency of the system. The natural frequency ω_0 is governed by the nonlinear term $\frac{3\alpha_1 D^2 \epsilon e^{\alpha_2 \epsilon t}}{8\omega_0}$, which depends on the amplitude D, damping ϵ, the parameters α_1, α_2, and the time t.

7.1.17 Comparison with Existing Literature

I conducted a comparative analysis with results from an established research paper. Despite the limitations and the absence of numerical methods my results were almost accurate to the results published in paper.

7.1.18 MATLAB plot of Analytical Solutions for Different Modes

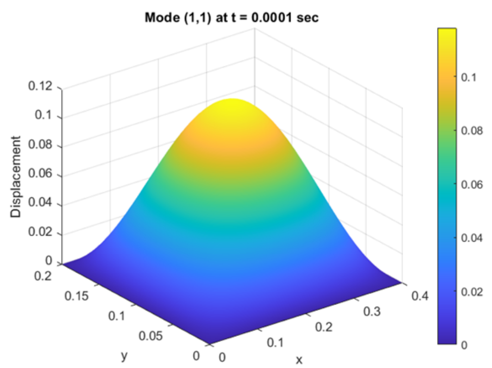

Figure 7.1: Analytical Vibration Mode (1,1) of the Non linear Rectangular Membrane

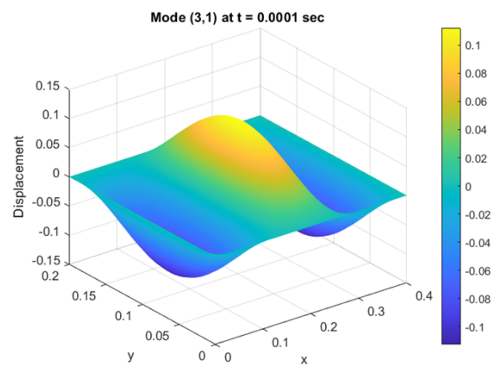

Figure 7.2: Analytical Vibration Mode (1,3) of the Non linear Rectangular Membrane

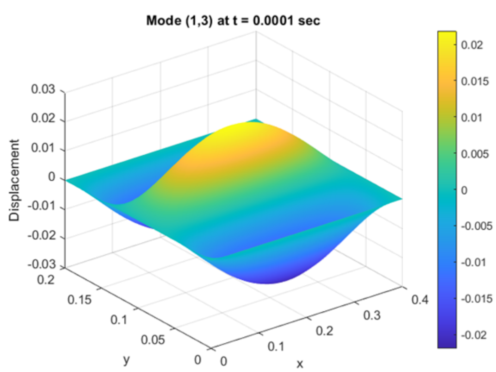

Figure 7.3: Analytical Vibration Mode (3,1) of the Non linear Rectangular Membrane

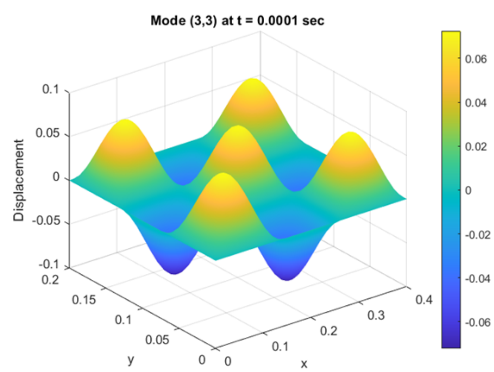

Figure 7.4: Analytical Vibration Mode (3,3) of the Non linear Rectangular

7.1.19 MATLAB Plot of Amplitude vs Time

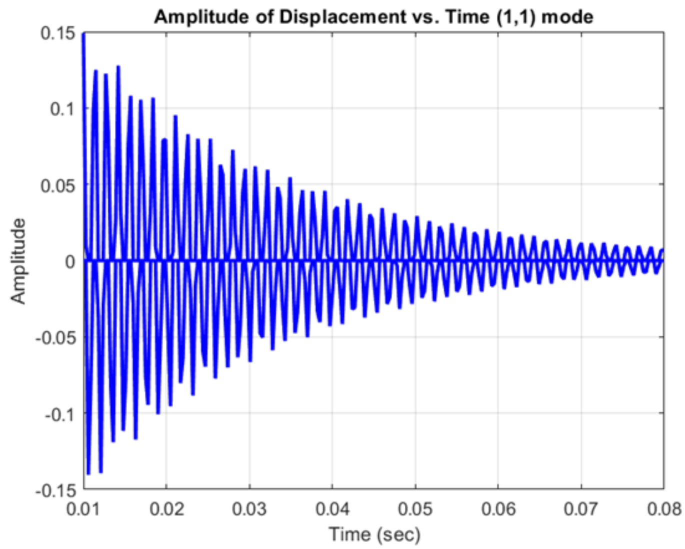

Figure 7.5: Plot of Amplitude vs Time for (1,1) mode

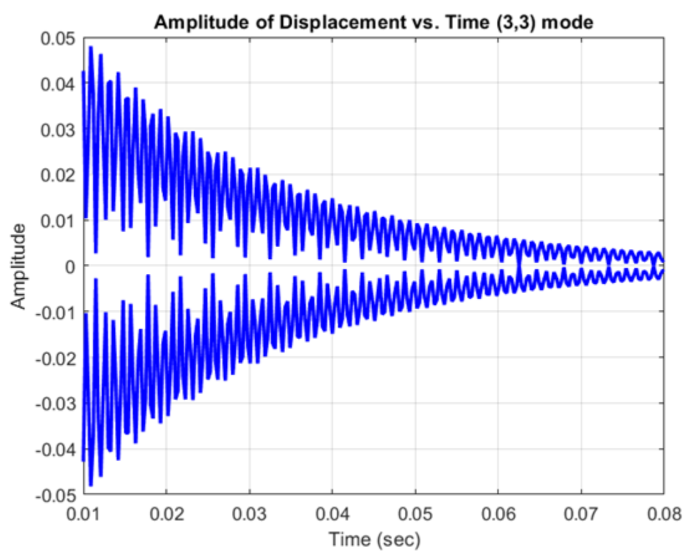

Figure 7.6: Plot of Amplitude vs Time for(3,3) mode

Chapter 8

Conclusions

This report provides a thorough analysis of the vibrational behaviour of membranes and linear and nonlinear SDOF. This study emphasises how difficult it may be to forecast a system's dynamic reaction in a variety of scenarios, especially when nonlinearities are present.

8.1 Linear SDOF Systems

This section serves as the study's cornerstone. The governing differential equations for both damped and undamped oscillators were first solved. Without damping, the system has been shown to exhibit simple harmonic motion, with an elliptical phase portrait indicating continuous kinetic and potential energy exchange inside the system. It was also determined how the oscillation's amplitude depended on the starting point and natural frequency.

A shift in the behaviour of the system was noted in the case of damping. The phase portrait underwent a transformation from an ellipse to a spiral, signifying the gradual depletion of energy. Underdamped systems exhibit an exponential decrease in oscillation amplitude. Additionally, the study offered a convincing justification and evidence for why the phase portrait takes on these shapes, linking the mathematical analysis to the physical behaviour of the system.

Additionally investigated was the connection between amplitude, initial displacement, initial velocity, and angular velocity. When developing systems that require control over vibrational behaviour, like tuned mass dampers or vibration isolation systems, these relationships are essential.

8.2 Nonlinear SDOF Systems

An additional level of complexity was brought about by the switch to nonlinear SDOF systems. Variable stiffness was the system's source of nonlinearity. For positive displacement, it was always positive, and for negative displacement, it was always zero. These kinds of stiffness can be found in **Tension stiffened structure**, where the material sags when there is no tension. Consider parachute systems.

Several important conclusions were obtained from the nonlinear system analysis. The system displayed damped oscillatory behaviour for positive displacements, which was more complicated than the linear case because the restoring force was non-constant. The damping effect caused the oscillation's amplitude to gradually drop, and the phase portrait revealed a spiralling track that led back to the origin.

The system exhibited a very distinct behaviour for negative displacements. Since there was no longer a restoring force, damping was the sole force affecting the system, which resulted in an exponential velocity decay without oscillation. The absence of oscillatory motion was reflected in the phase portrait for this region, which had a trajectory that quickly reached the origin. This behaviour emphasises how crucial restoring forces are to maintaining oscillations and how difficult it is to analyse systems in which the restoring force is conditional.

The forced nonlinear SDOF system, in which the dynamics of the system were altered by an outside force, was also examined in this study. The system became much more complex, especially when there were both periodic and random components in the external force. It was difficult to solve this issue analytically, thus numerical techniques were used utilising MATLAB's ODE45 solver. The outcomes demonstrated that the mass, stiffness, damping, and beginning circumstances all had a significant impact on the system's reaction. We found through a parametric research that the system's natural frequency rose with increasing stiffness and fell with increasing mass. When included in the external force term, the damping coefficient affected the rate of energy dissipation but had a complicated connection with the natural frequency.

8.3 Membrane Vibration Analysis

The examination of membrane vibrations gave the analysis a new perspective. Membranes are more sensitive to starting tension and boundary conditions than beams and shells because they can only withstand loads through tension. Analytical and numerical methods were employed to analyse membranes that were circular, elliptical, and rectangular while they were in free vibration.

Mathieu functions have been utilised to derive the analytical solutions for elliptical membranes and Bessel functions for circular membranes . These solutions aid in the estimation of modes as well as the natural frequency for various modes. Next, the finite difference method was employed in MATLAB to provide numerical solutions. The accuracy of the numerical method was then confirmed by comparing it with an analytical solution.

The study demonstrated the critical significance that initial tension plays in maintaining oscillatory behaviour in membranes. By introducing initial tension, compression is avoided and a constant restoring force is maintained since the membrane is kept under tension even during negative displacements. This behaviour contrasts sharply with beams and shells, where geometric shapes and material qualities affect the restoring force.

Additional understanding of the dynamic response of membranes was obtained through the nonlinear study of membrane vibrations under impact loading. The investigation revealed that the large amplitude oscillations and the impact of damping were major variables. Through the utilisation of D'Alembert's principle and von Kármán's large deflection theory, the study deduced approximate solutions for the nonlinear differential equations that regulate membrane vibrations. The findings demonstrated that the initial impact and the intrinsic characteristics of the membrane had a significant impact on the membrane's amplitude, frequency, and overall behaviour.

Almost correct findings were obtained when the analytical results were plotted and validated against available literature, despite the hurdles presented by the nonlinear system's complexity.

8.4 Overall Insights

- Provides a detailed analysis of both linear and nonlinear SDOF systems.
- Emphasizes on excitation of higher harmonics in SDOF due to non linearities.
- Provides a detailed analysis of free vibration of membranes.
- Emphasizes the critical role of initial tension in membrane dynamics, offering valuable insights for the design of membrane-based structures.
- Also provides analytical perspective of non linear vibration of membrane.

Bibliography

[1] H. Minami, “Added mass of a membrane vibrating at finite amplitude,” *Journal of Fluids and Structures*, 1998.

[2] C. Liu, Z. Zheng, X. Yang, and H. Zhao, *Nonlinear Damped Vibration of Pre-Stressed Orthotropic Membrane Structure under Impact Loading*. World Scientific Publishing Company, 2014.

[3] Q. Guo, *Solution for Free Vibration Problem of Membrane with Unequal Tension in Two Directions*. Wuhan, China: HUST Press, 1982.

[4] S. S. Rao, *Mechanical Vibrations*, 5th ed. Pearson, 2010.

[5] S. H. Strogatz, *Nonlinear Dynamics and Chaos: With Applications to Physics, Biology, Chemistry, and Engineering*, 2nd ed. Westview Press, 2015.